Extended MHD Studies with the M3D-C^1 Code

Presented by S. C. Jardin
PPPL Theory Research and Review Seminar
April 18, 2014

- M3D-C^1 Code
  - equations solved
  - code features
  - code options
- Physics studies in progress
- Future plans
  - new physics studies
  - new code capabilities

Nate Ferraro (GA)
Josh Breslau
Jin Chen
Brendan Lyons
Jesus Ramos (MIT)
Isabel Krebs (IPP)
Stuart Hudson
Mark Shephard (RPI)
Fan Zhang (RPI)
Lucca Guzzatto (UR)
Stefan Gerhardt
H. Park (KSTAR)
S Sabbagh (CU)
Linda Sugiyama (MIT)
Hank Strauss (HRS)
Guoyong Fu

M3D-C^1 solves the three-dimensional two-fluid MHD equations in a magnetized torus:

$$\frac{\partial n}{\partial t} + \nabla \bullet (n\mathbf{V}) = 0$$

$$\frac{\partial \mathbf{B}}{\partial t} = -\nabla \times \mathbf{E} \qquad \mathbf{B} = \nabla \times \mathbf{A} \qquad \mathbf{J} = \nabla \times \mathbf{B}$$

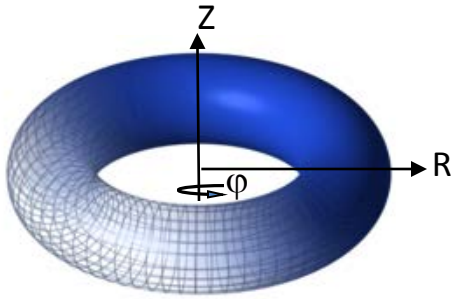

$$nM_i\left(\frac{\partial \mathbf{V}}{\partial t} + \mathbf{V} \bullet \nabla \mathbf{V}\right) + \nabla \bullet \mathbf{P} = \mathbf{J} \times \mathbf{B} - \nabla \bullet \boldsymbol{\Pi}_{GV} + \mu \nabla^2 \mathbf{V}$$

$$\mathbf{E} + \mathbf{V} \times \mathbf{B} = \mathbf{R}_c + \frac{1}{ne}\left(\mathbf{J} \times \mathbf{B} - \nabla \bullet \mathbf{P}_e\right) - \lambda_H \nabla^2 \mathbf{J}$$

$$\frac{3}{2}\frac{\partial p_e}{\partial t} + \nabla \bullet \left(\frac{3}{2} p_e \mathbf{V}\right) = -p_e \nabla \bullet \mathbf{V} + \eta J^2 + \frac{\mathbf{J}}{ne} \bullet \left[\frac{3}{2}\nabla p_e - \frac{5}{2}\frac{p_e}{n}\nabla n\right] - \nabla \bullet \mathbf{q}_e + Q_\Delta$$

$$\frac{3}{2}\frac{\partial p_i}{\partial t} + \nabla \bullet \left(\frac{3}{2} p_i \mathbf{V}\right) = -p_i \nabla \bullet \mathbf{V} + \mu \left|\nabla V\right|^2 - \nabla \bullet \mathbf{q}_i - Q_\Delta$$

Resistive MHD: $\nabla \bullet \mathbf{P} = \nabla p, \ \mathbf{R}_c = \eta \mathbf{J}$

2-fluid terms

Kinetic closures extend these to include neo-classical, energetic particle, and turbulence effects.

Features of the M3D-C^1 code

- High accuracy
  - High order finite elements in 3D
  - Optimal decomposition of vector fields into scalars: $\nabla \bullet \mathbf{B} \equiv 0$
  - Full 2F MHD equations: accurate treatment of $\nabla \bullet \chi_{||} \mathbf{bb} \bullet \nabla T_e$
  - Accuracy of linear flux-coordinate (FC) codes without using FC

- Can perform long-time simulations: $t > 10^4 - 10^5\ \tau_A$ (~10 ms)
  - Made possible by efficient fully implicit time-advance algorithm
  - Allows study of stability on the transport timescale
    - Approach to instability boundary
    - Full sawtooth (and ELM?) cycle …. Buildup and crash

- Geometrical flexibility
  - Unstructured mesh allows variable mesh size (mesh packing)
  - Plasma region with seperatrix (free boundary)
  - Arbitrary shaped (finite thickness) vacuum vessel and conductors
  - Straight cylinder or torus

Features of the M3D-C^1 code

- High accuracy
  - High order finite elements in 3D

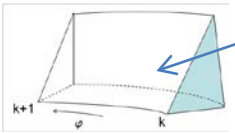

Within each element, each scalar field is represented as a polynomial in (R,φ,Z) with 72 terms. All first derivatives are continuous.

  - Optimal decomposition of vector fields into scalars: $\nabla \bullet \mathbf{B} \equiv 0$
  - Full 2F MHD equations: accurate treatment of $\nabla \bullet \chi_{||} \mathbf{bb} \bullet \nabla T_e$
  - Accuracy of linear flux-coordinate (FC) codes without using FC

- Can perform long-time simulations: $t > 10^4 - 10^5\ \tau_A$ (~10 ms)
  - Made possible by efficient fully implicit time-advance algorithm
  - Allows study of stability on the transport timescale for realistic η
    - Approach to instability boundary
    - Full sawtooth (and ELM?) cycle …. Buildup and crash

- Geometrical flexibility
  - Unstructured mesh allows variable mesh size (mesh packing)
  - Plasma region with seperatrix (free boundary)
  - Arbitrary shaped (finite thickness) vacuum vessel and conductors
  - Straight cylinder or torus

M3D-C^1 code compilation options

- Full 3D nonlinear
  - High order finite elements in 3D
  - Can evolve equilibrium state or hold 2D equilibrium fixed
  - For evolving equilibrium mode, need to specify transport model, current control systems, particle and energy sources, etc
  - 64-12000+ processors

- 2D nonlinear
  - Same code as 3D nonlinear, but $\partial/\partial\varphi \equiv 0$
  - Runs very fast on 8-16 processors
  - Very useful for scoping transport model, control systems, etc

- 3D linear
  - Same code, but all quantities are complex: $\partial/\partial\varphi \rightarrow i\, n\, \varphi$
  - Runs very fast on 8-16 processors
  - Very well benchmarked for ideal and resistive stability

The 3 versions are obtained with different compiler directives.

M3D-C^1 code model options

$$\mathbf{V} = R^2 \nabla U \times \nabla \varphi + \omega R^2 \nabla \varphi + R^{-2} \nabla_\perp \chi$$

$$\mathbf{A} = R^2 \nabla \varphi \times \nabla f + \psi \nabla \varphi - F_0 \ln R \hat{Z}$$

(R,φ,Z) are cylindrical coordinates

- Most complete full 2F model advances 8 scalars in time:

$$\mathbf{Y}(R,\varphi,Z,t) = \left[U, \omega, \chi, \psi, f, p_e, p_i, n\right]$$

- Simplest reduced MHD model advances only 2 scalars:

$$\mathbf{Y}(R,\varphi,Z,t) = \left[U, \psi\right]$$

- Many intermediate options available: 2 → 8 scalars

Reduced models run very fast and can be used for scoping studies or to elucidate physics

M3D-C^1 Physics Studies in Progress

- Two-fluid reconnection in simple geometry
- Repeating sawtooth and stationary states
- Double tearing modes
- H-Mode pedestal formation
- Soft-beta limit and saturated modes
- Neoclassical tearing modes
- Disruption studies and resistive wall modes
- ELM studies and RMP
- NTV Studies
- LZ+JB Test problem

M3D-C^1 Physics Studies in Progress

- Two-fluid reconnection in simple geometry
- Repeating sawtooth and stationary states
- Double tearing modes
- H-Mode pedestal formation
- Soft-beta limit and saturated modes
- Neoclassical tearing modes
- Disruption studies and resistive wall modes
- ELM studies and RMP
- NTV Studies
- LZ+JB Test problem

Two-fluid reconnection in simple geometry

J for nonlinear benchmark problem

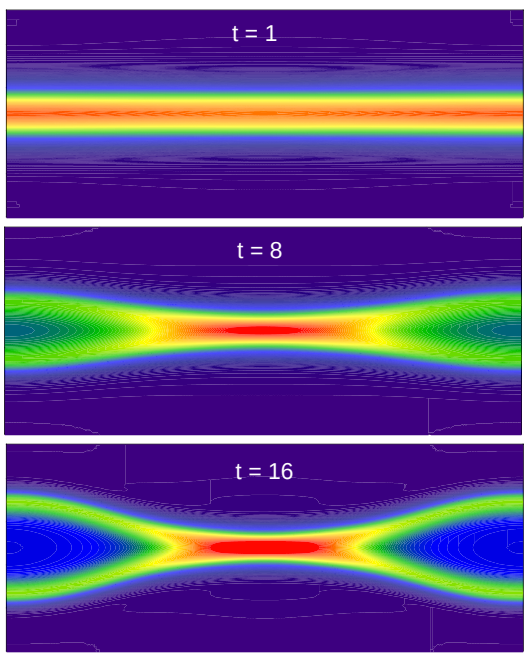

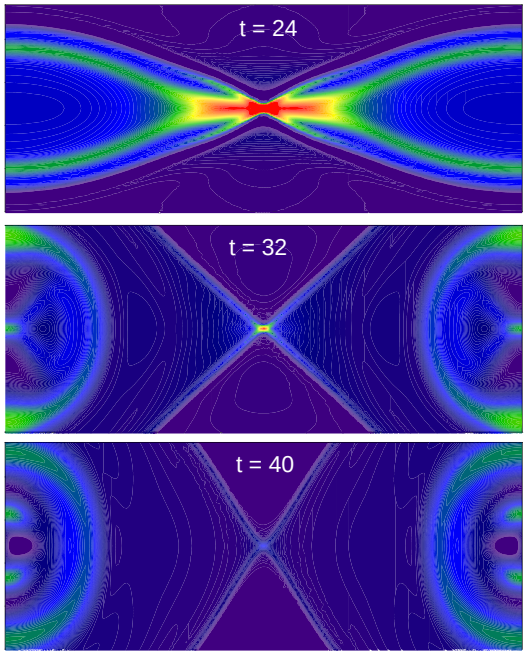

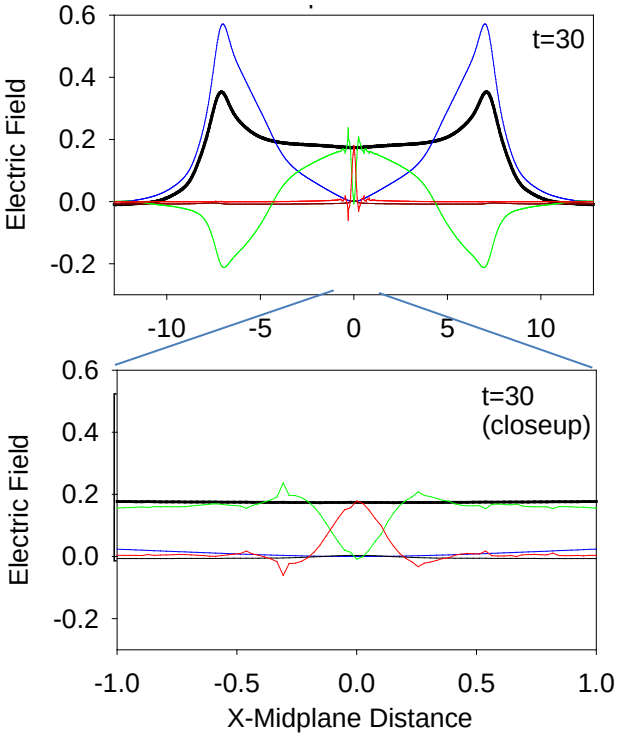

Clarified 2F reconnection physics. λ_H is necessary mathematically, but rate is independent of λ_H for λ_H sufficiently small.

$$\mathbf{E} = -\mathbf{V}\times\mathbf{B} + \eta\mathbf{J} + \frac{1}{ne}\mathbf{J}\times\mathbf{B} - \lambda_H\nabla^2\mathbf{J}$$

M3D-C^1 Physics Studies in Progress

- Two-fluid reconnection in simple geometry
- Repeating sawtooth and stationary states
- Double tearing modes
- H-Mode pedestal formation
- Soft-beta limit and saturated modes
- Neoclassical tearing modes
- Disruption studies and resistive wall modes
- ELM studies and RMP
- NTV Studies
- LZ+JB Test problem

We are using M3D-C^1 to solve the MHD equations to compute the self-consistent long-time (transport timescale) behavior of a tokamak discharge subject to:

- loop voltage (I_P controller)
- density source (n_e controller)
- heating source (NB)
- momentum source (NB)
- shaping fields

- resistivity η
- viscosity ν
- thermal conductivity $\kappa_{||}$ & $\kappa_{\perp}$
- particle diffusivity D
- ion-skin depth $d_i = c/\omega_{pi}$

Standard transport model:

$$\eta = \eta_0 \left(\frac{T_e}{T_{e0}} \right)^{-3/2} \qquad \nu, D = \text{const} \qquad \kappa_{\perp} = \kappa_0 \left[1 + \alpha \left| \nabla T_e^2 \right| \right] \left(\frac{p}{p_0} \right)^{-1/2} \qquad \kappa_{||} \simeq 10^5 \kappa_0$$

Initial conditions have $q_0 < 1$, so one sawtooth always occurs.

Can we quantitatively model full repeating sawtooth cycles?
Under what circumstances do sawteeth disappear and why?

Typical periodic oscillations $S=10^6$, $\beta=.001$

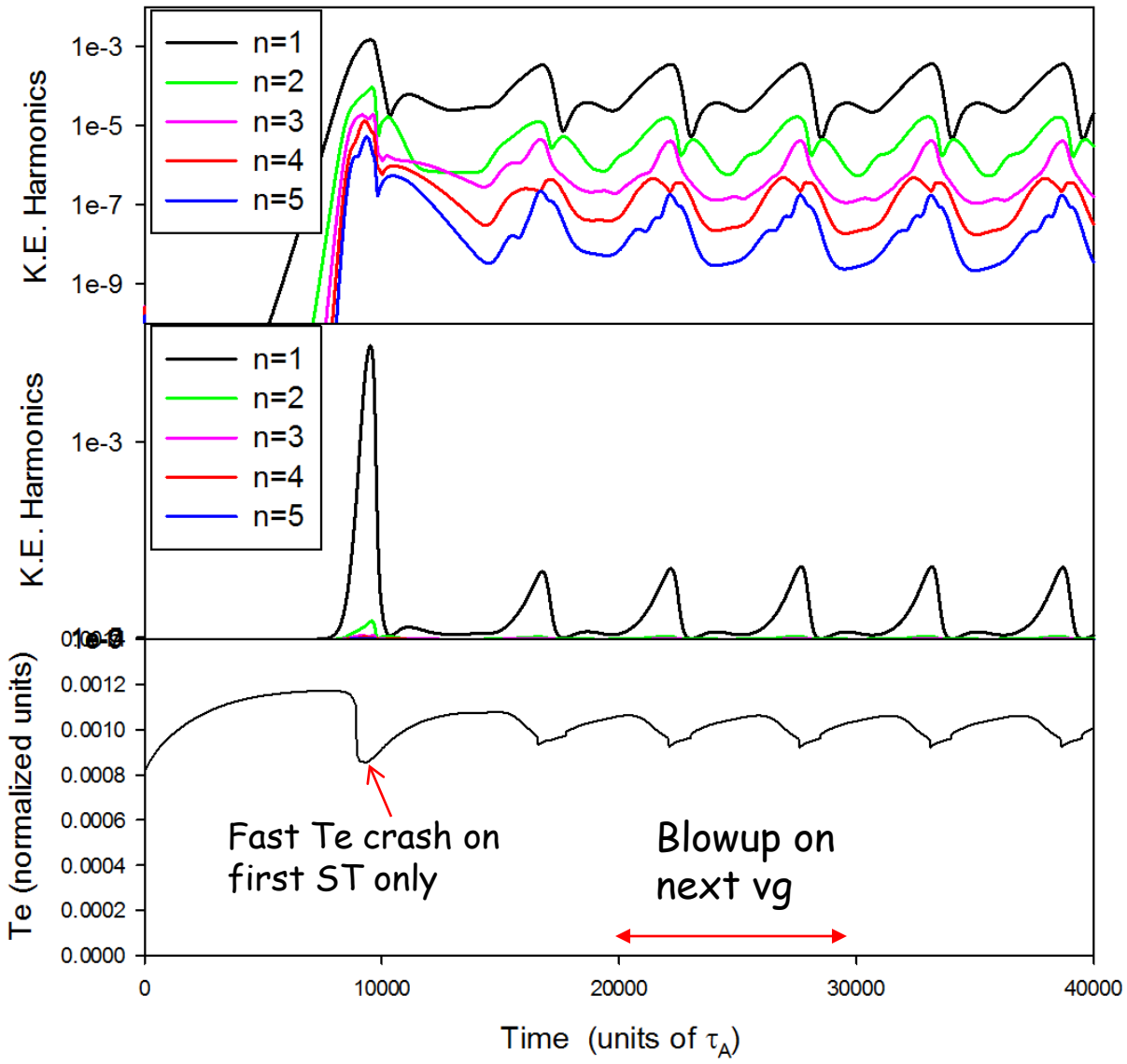

At low β, low S, resistive MHD plasma exhibits periodic oscillations, but does not show repeating fast Te crashes

CMOD 16G

Kadomsev complete reconnection S=10^6 β=.001

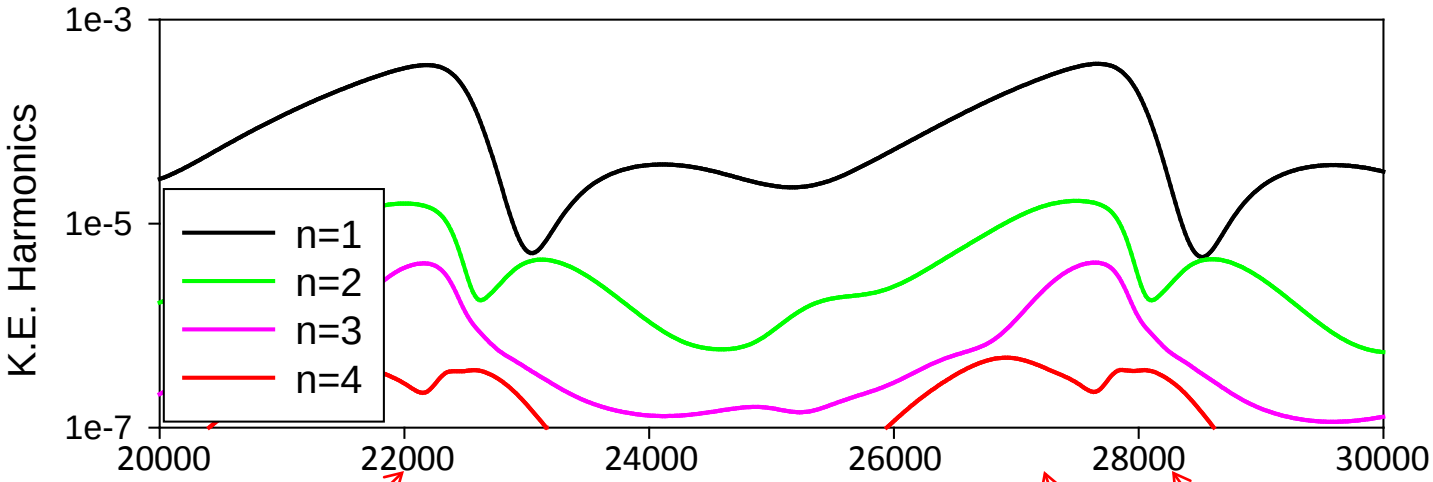

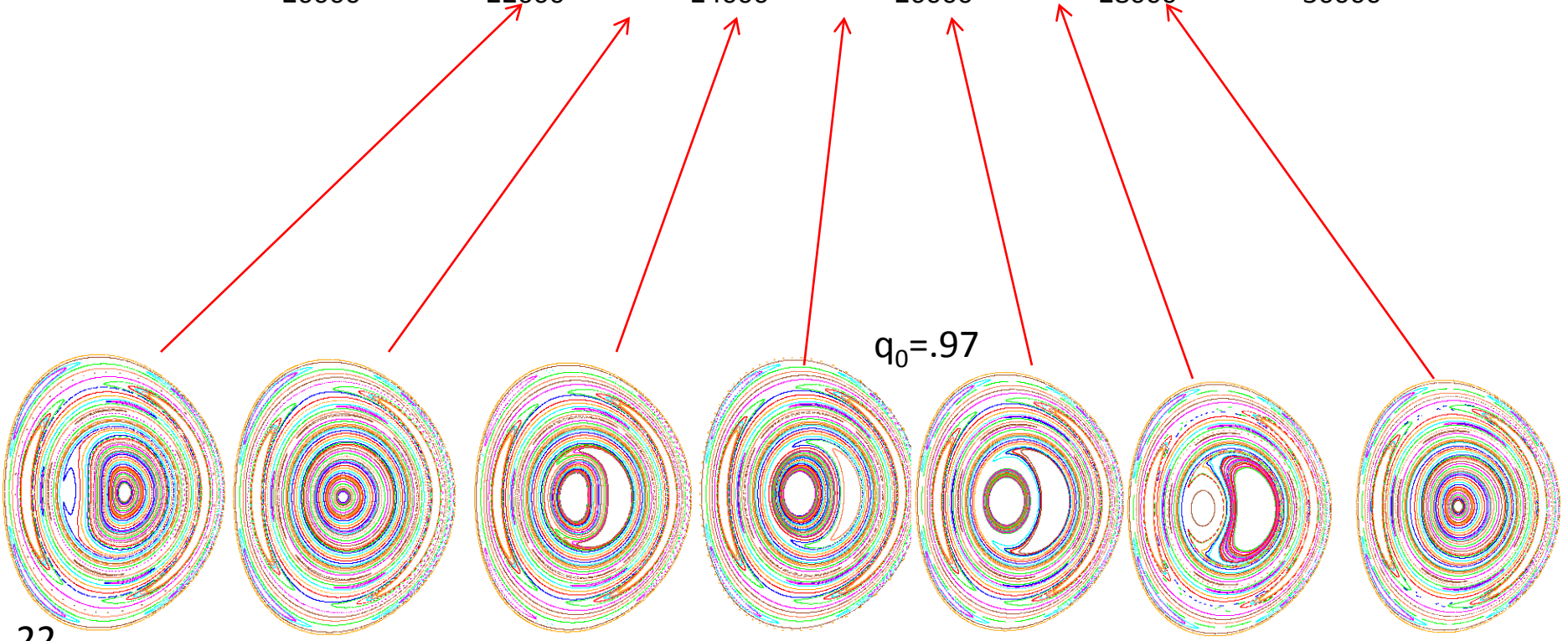

Resistivity scan: $\beta = .001$, no rotation

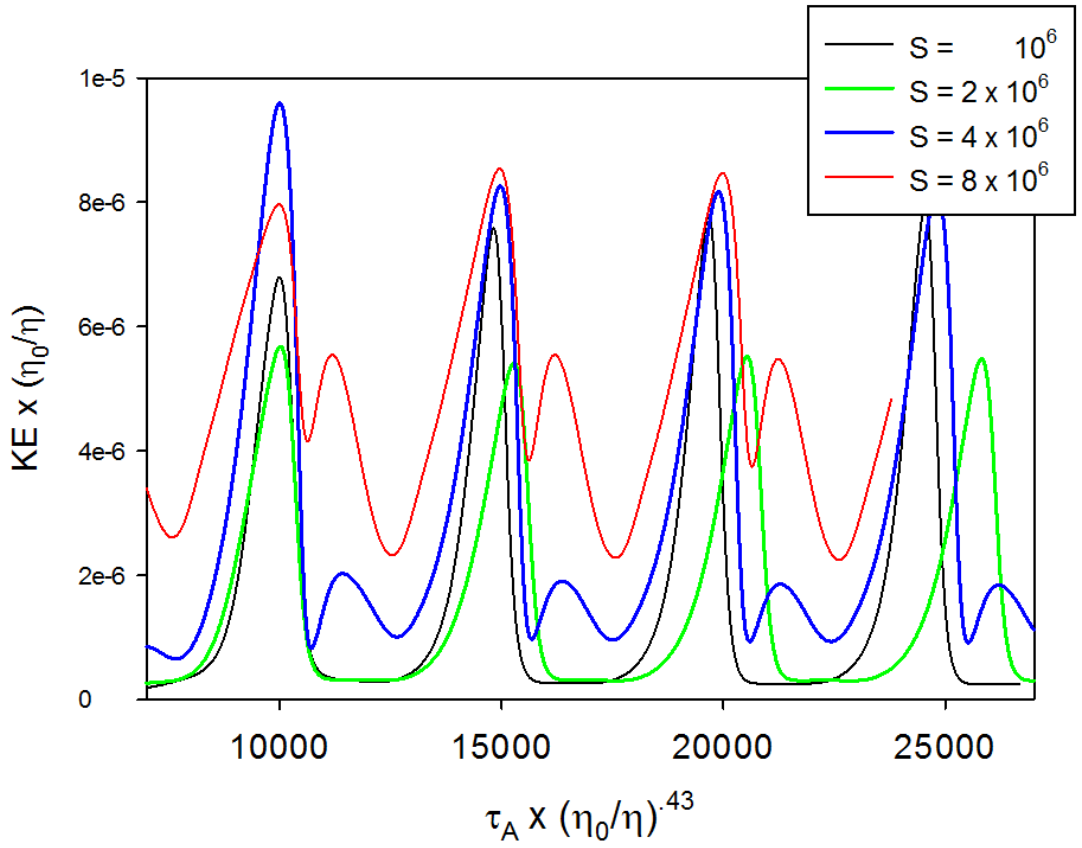

- period gets longer as η gets smaller as $\eta^{-0.43}$
- kinetic energy per event decreases as η

- Δq_0 decreases from 0.05 to < 0.01 as η decreases :
- Complete Kadomsev reconnection does not occur at high S
- Evidence of incomplete reconnection but fast Te crash at high S (2F)

CMOD07 μ = 10 E-5
CMOE09 μ = 10
CMOD29 μ = 2.5
CMOD1E μ = 1.0

Comparison of resistive MHD and 2F MHD

Two simulations with same β=.001 and S=10^6: with and without 2F terms

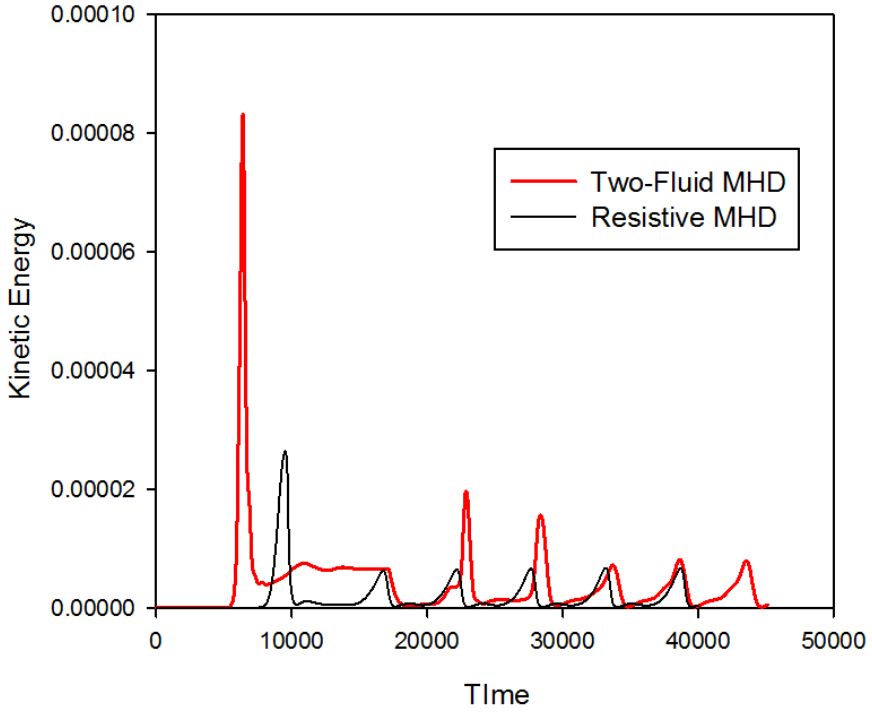

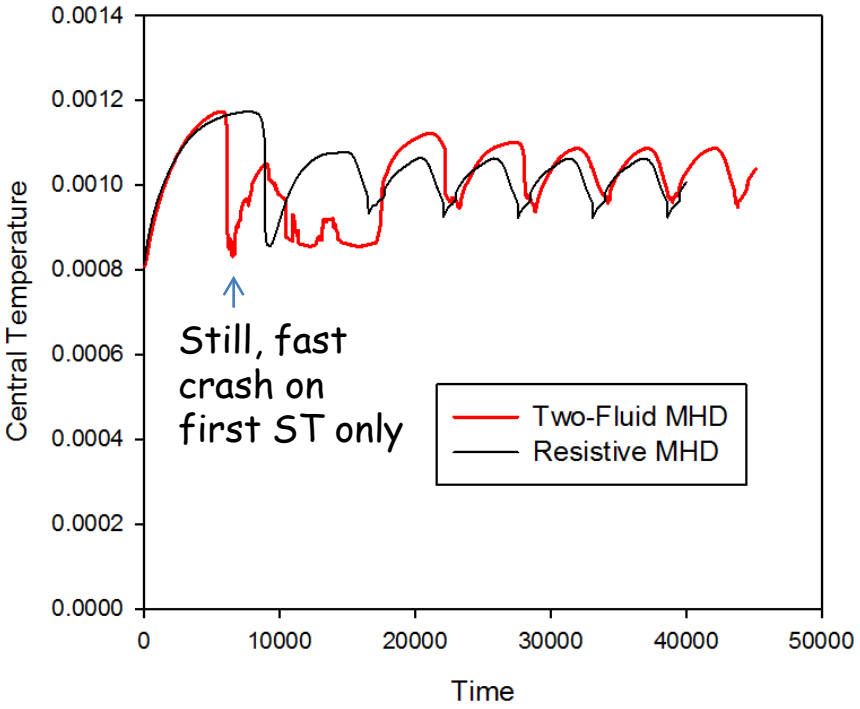

Two-fluid terms change the initial behavior, but not the long-time behavior of repeating sawteeth at low β and low S=10^6.

CMOD16G
CMOD25G

β=0.5% $S=10^6$
-- oscillations die out to form stationary state

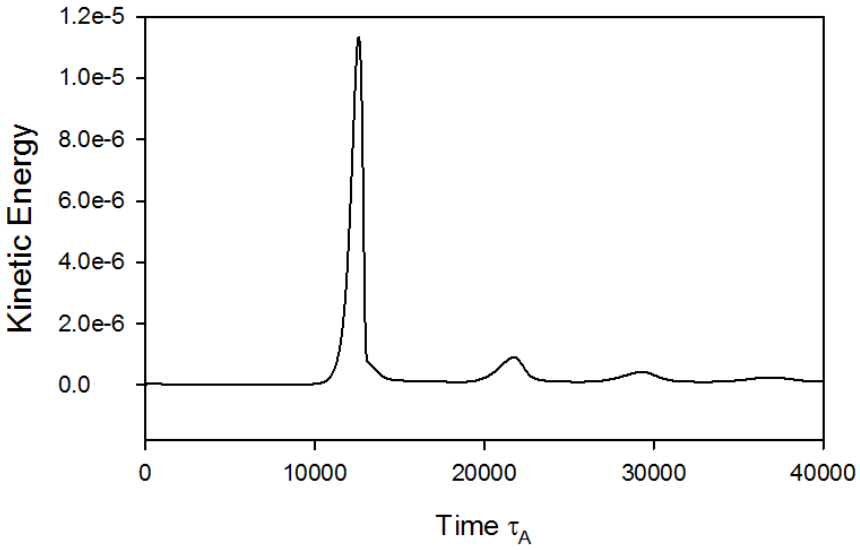

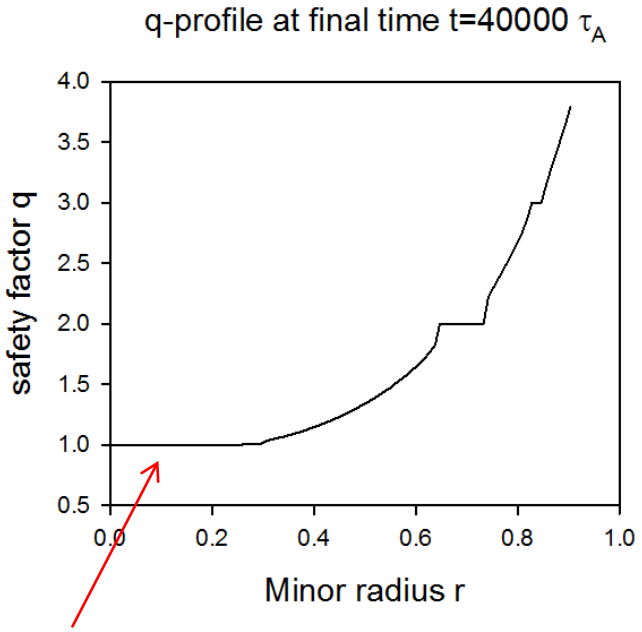

Large region in center with $q = 1 + \varepsilon$

At higher values of β , periodic oscillations die out and a stationary interchange mode develops with q just above 1 in a large volume near the axis ($S = 10^6$)

CMOD15 μ=10
Also, see
CMOD02
CMOD11
CMOD35

Stationary state has flattened current profile

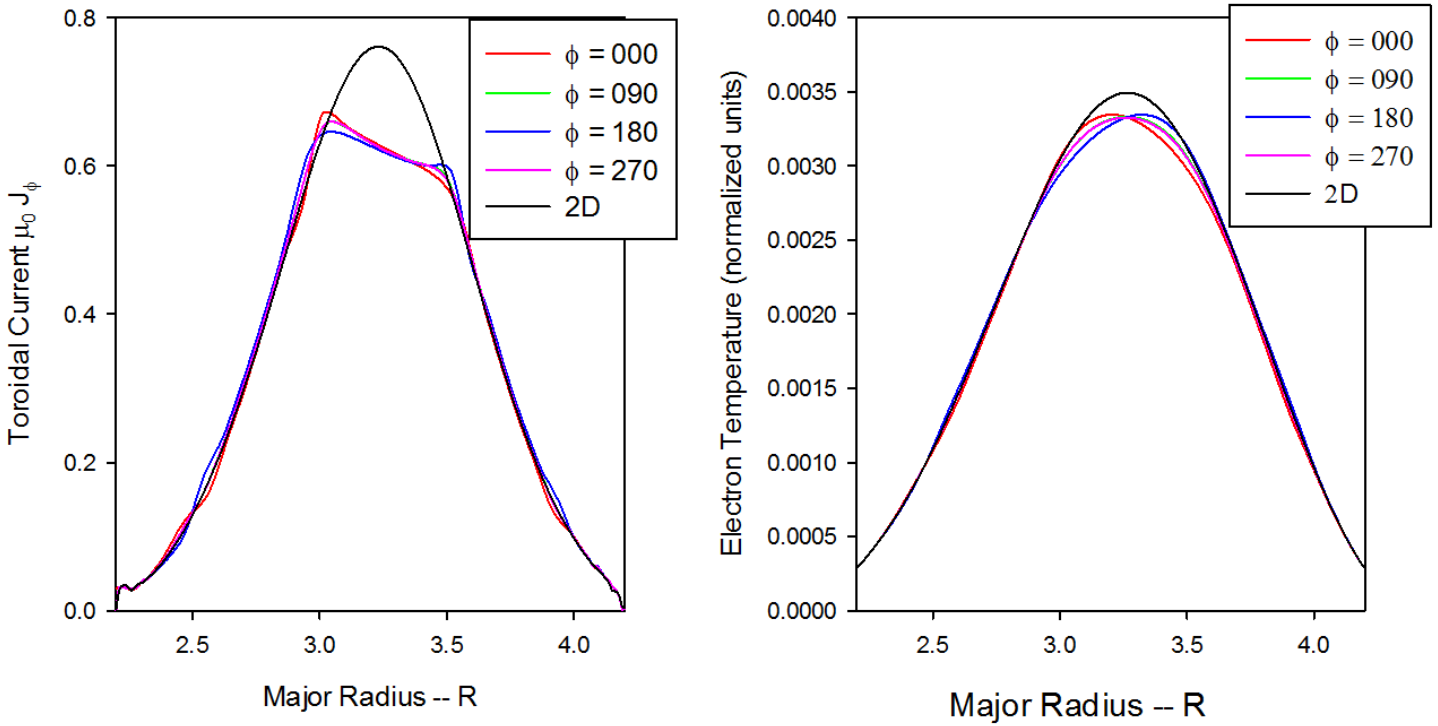

Comparison of slices of the 3D current and temperature profiles with results from a 2D calculation shows that the stationary interchange instability acts to flatten the current and temperatures near the center…keeping $q_0 \sim 1$

run15

Central poloidal flow flattens current profile

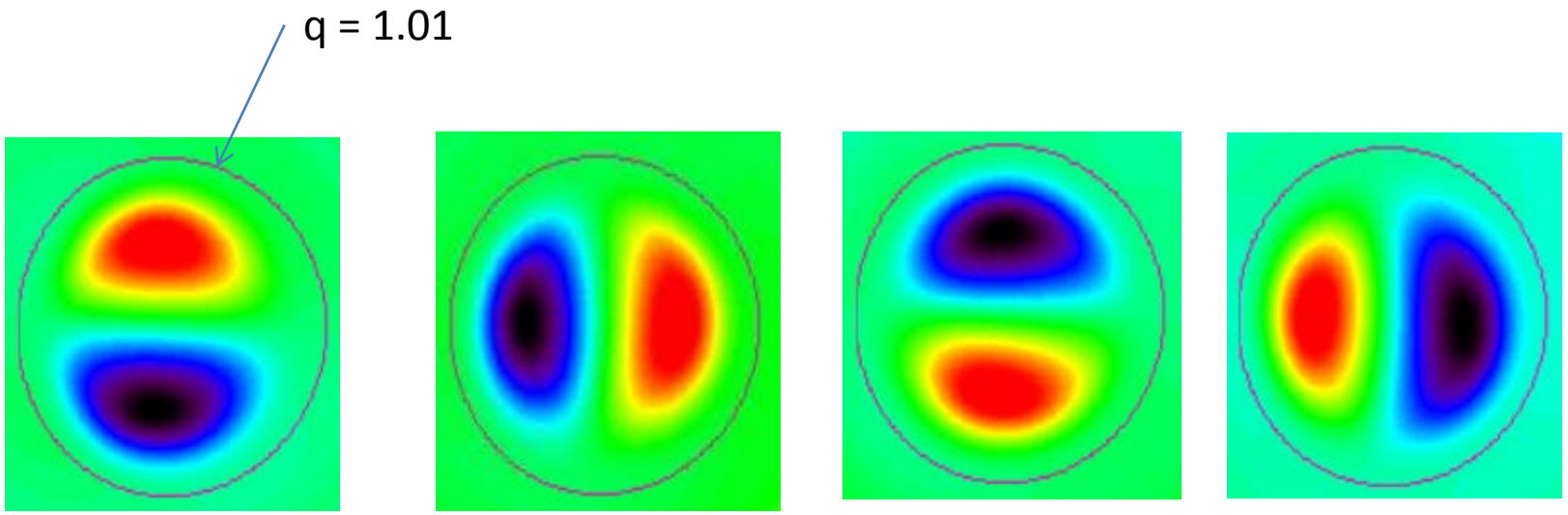

$\varphi = 0^0$ $\varphi = 90^0$ $\varphi = 180^0$ $\varphi = 270^0$

Contours of poloidal velocity stream function U at final time shows a clear (1,1) structure that is stationary in time.

Hill's vortex like flow pattern in center

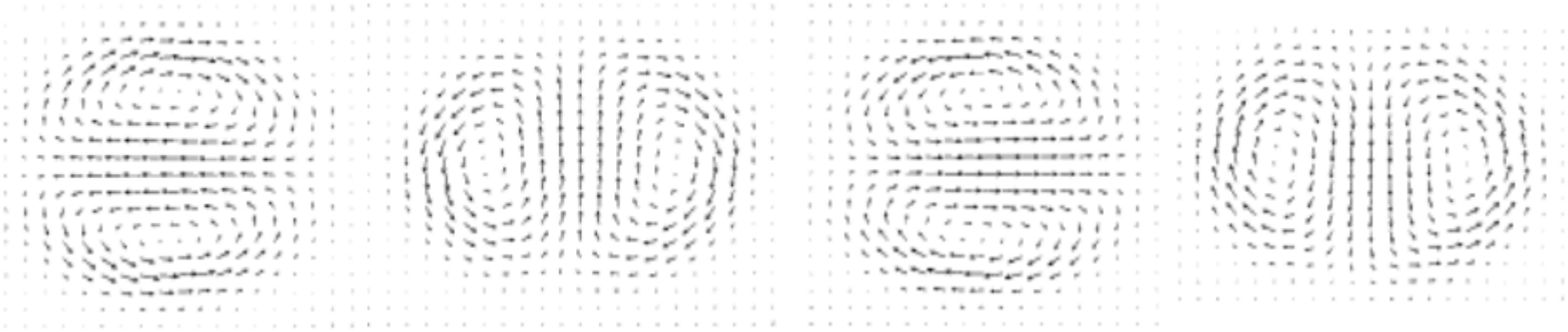

$\varphi = 0^0$ $\varphi = 90^0$ $\varphi = 180^0$ $\varphi = 270^0$

This stationary flow pattern is being driven by the interchange instability. It is also acting to flatten the temperature and current profiles to keep the central q=1 region stationary in time.

First 2F sawtooth shows distinctive shape

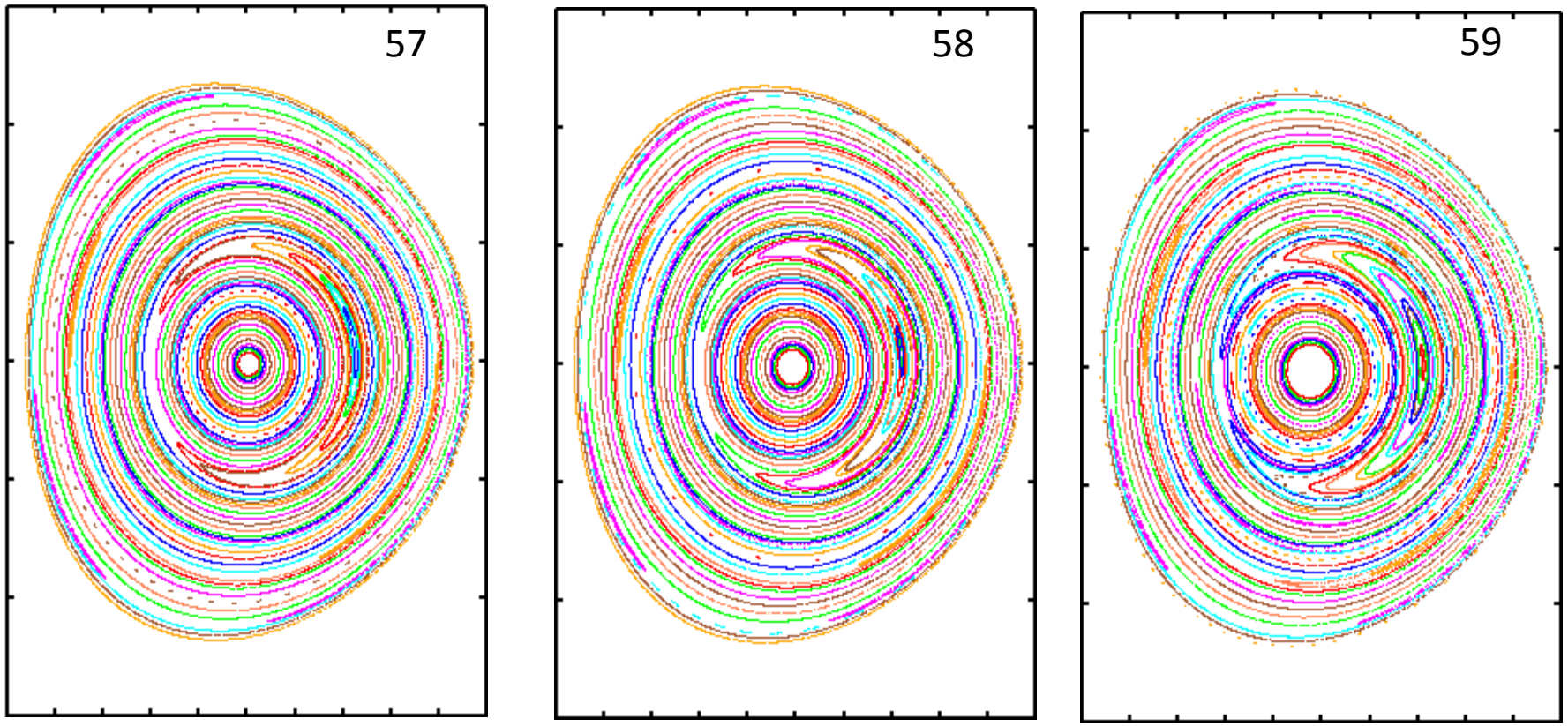

Compared to resistive MHD, in 2F sawtooth reconnection, the central surfaces are more circular and the reconnection layer is much shorter…leading to faster reconnection

CMOD run25

Surfaces are destroyed in reconnection region during temperature crash

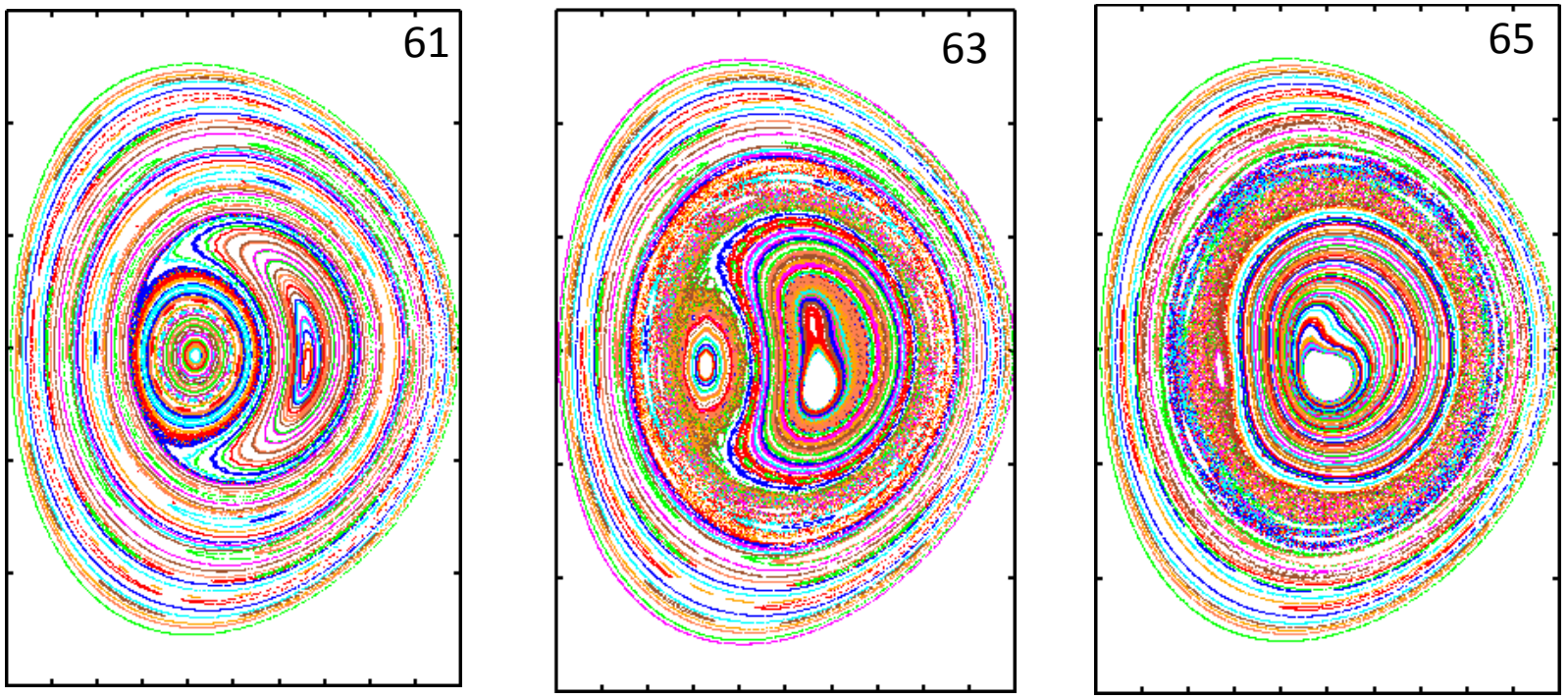

In 2F sawtooth reconnection, both the reconnecting plasma and the development of a stochastic layer at the q=1 surface contribute to the temperature crash.

CMOD run25

High S reconnection in cylindrical geometry

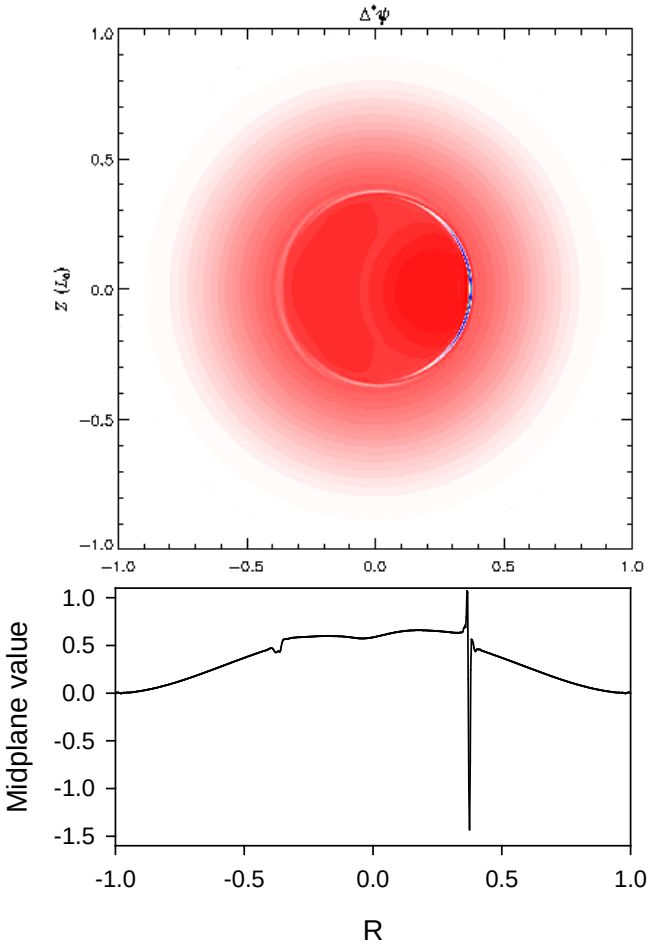

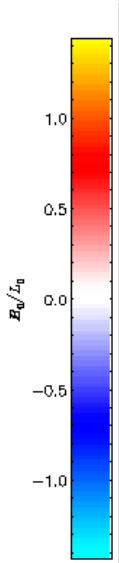

$S=\eta^{-1} = 10^8$

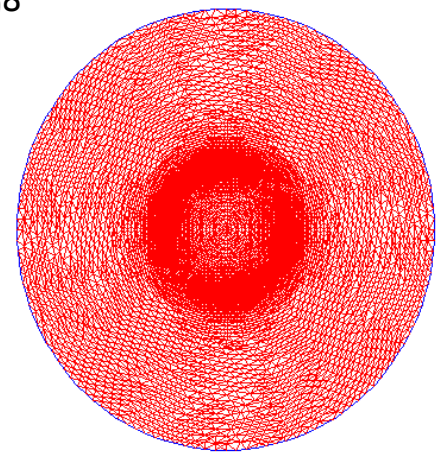

Adapted Mesh

Objective is to compare with high resolution 2D (helical) calculations where plasmoids were formed for sufficiently high $S > 10^8$

Isabel Krebs: MPCC

M3D-C^1 Physics Studies in Progress

- Two-fluid reconnection in simple geometry
- Repeating sawtooth and stationary states
- Double tearing modes
- H-Mode pedestal formation
- Soft-beta limit and saturated modes
- Neoclassical tearing modes
- Disruption studies and resistive wall modes
- ELM studies and RMP
- NTV Studies
- LZ+JB Test problem

Double Tearing Modes

Equilibrium current density

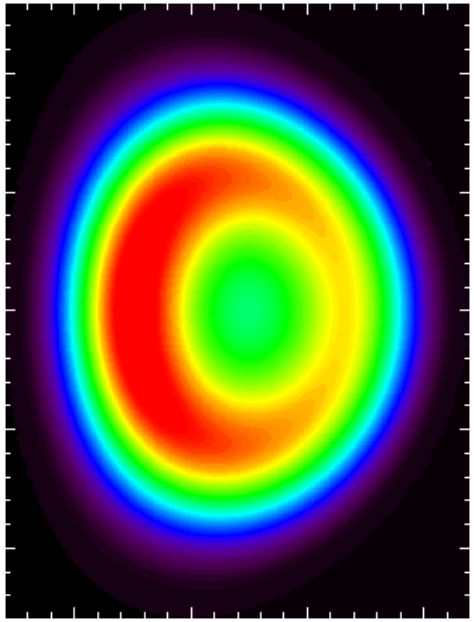

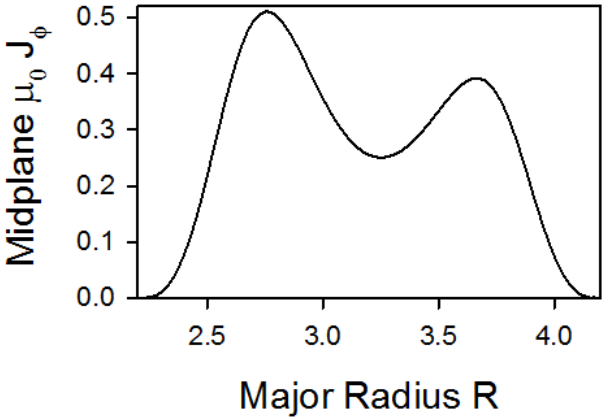

η= 1.E-7, β = 0.1%

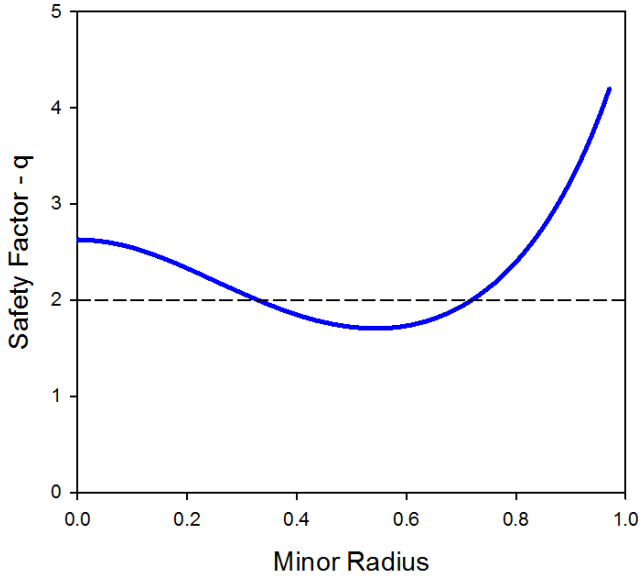

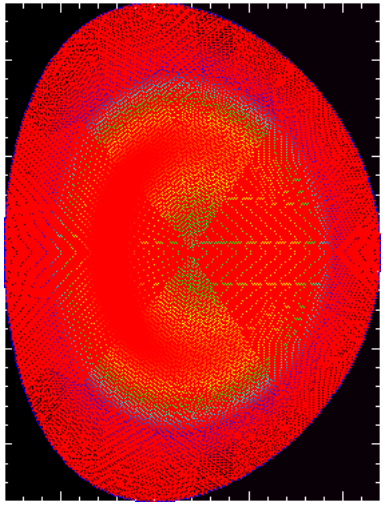

fixed boundary, uniform mesh

Goal is to understand when plasma is unstable to double tearing when there are two q=2 surfaces in plasma.

And, what is the nonlinear development?

Double Tearing Modes - cont

Normal displacement

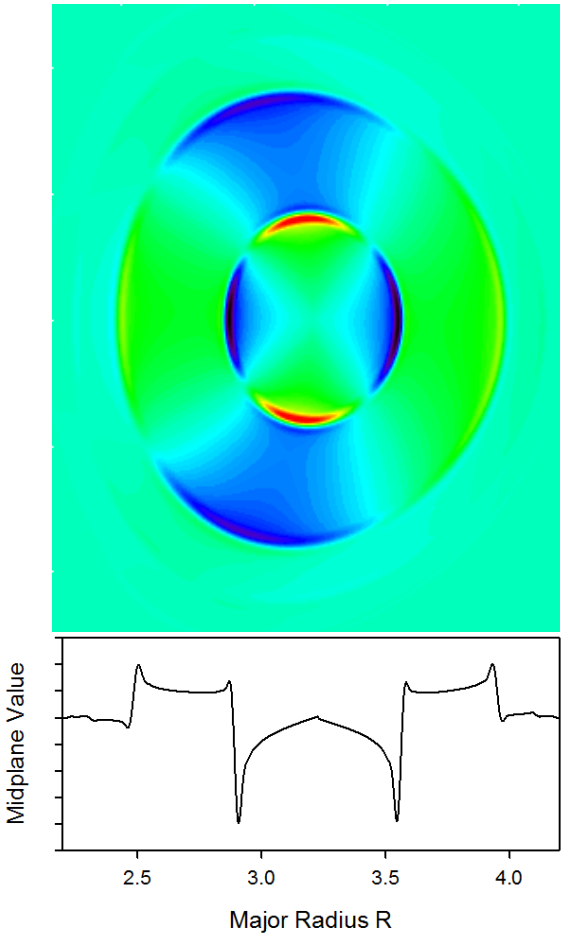

Perturbed current

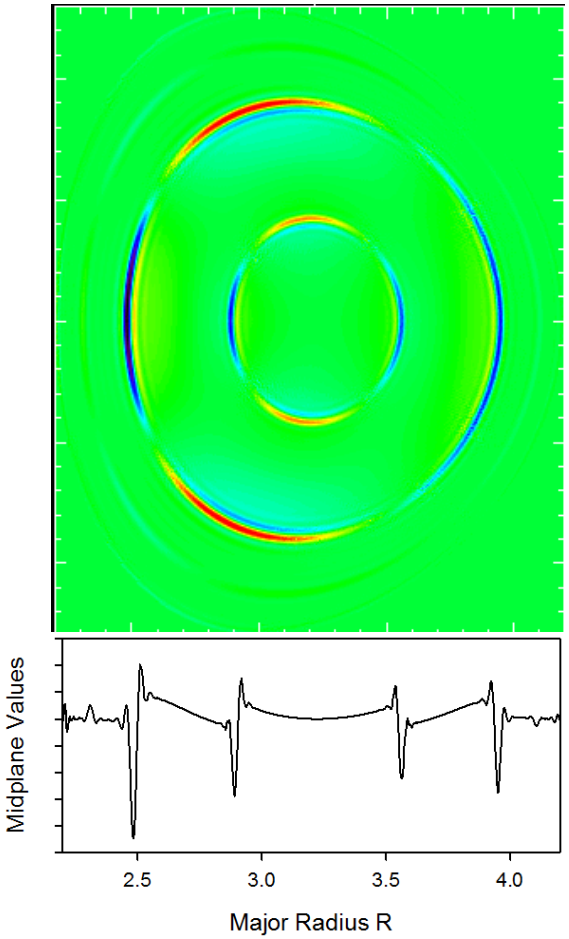

Poincare Plot

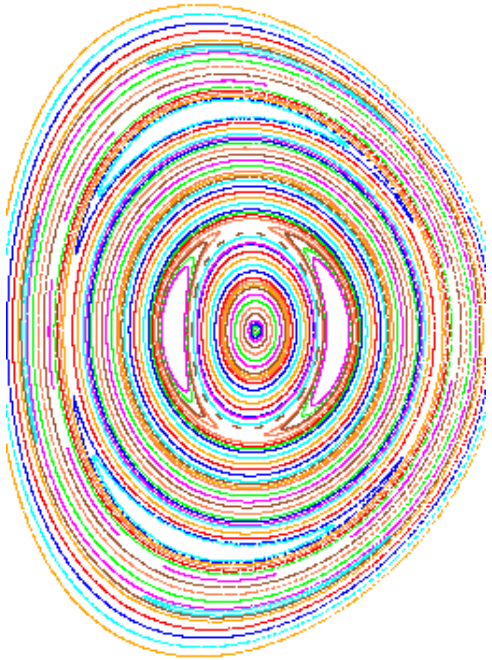

Linear eigenmode of double (2,1) tearing mode

To do:

- adaptive mesh
- scan NSTX parameters
- add sheared rotation
- onset conditions
- nonlinear evolution

Double Tearing Modes – q=1

Discharges with ECCD near center are thought to form multiple q=1 surfaces

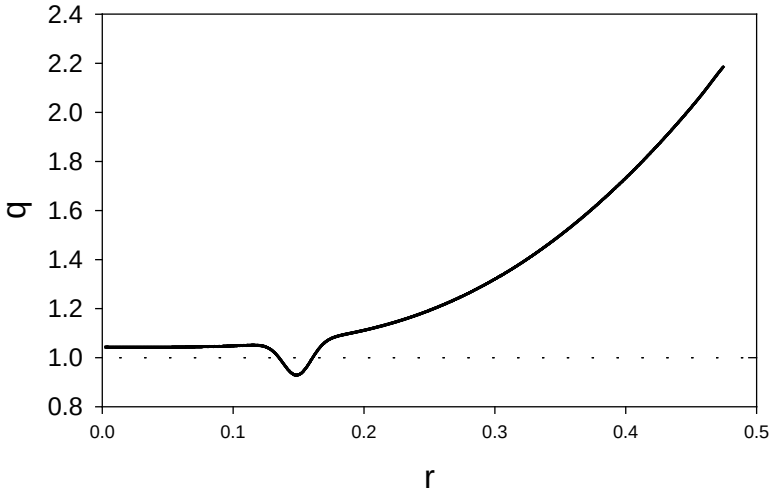

Adapted mesh refined for q < 1

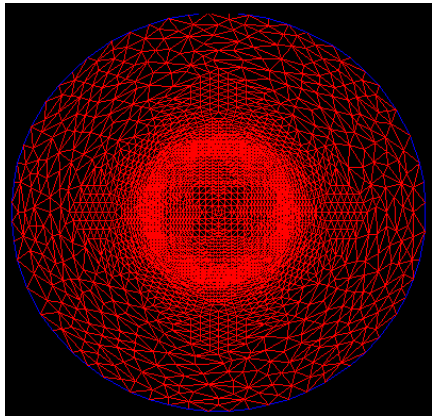

- M3D-C1 nonlinear simulation:
- Reduced MHD
- Straight system
- Equilibrium subtracted out
- 32 toroidal planes

n=4 most unstable first, n=5 later

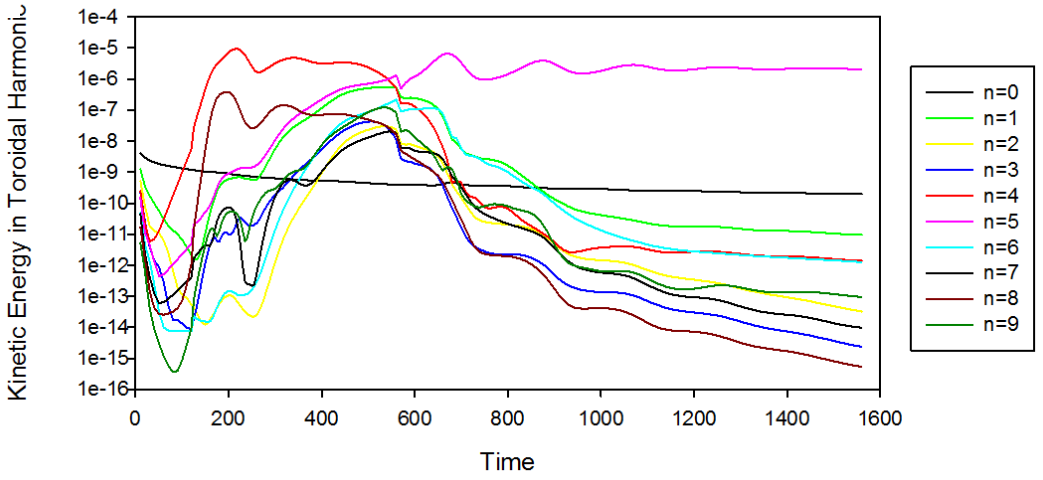

H. Park, et al…..KSTAR

Double Tearing Modes – q=1

Poloidal mode structure changes nonlinearly.

t = 185. m=7 t = 1600. m=9

U

$J_z = \nabla^2 \psi$

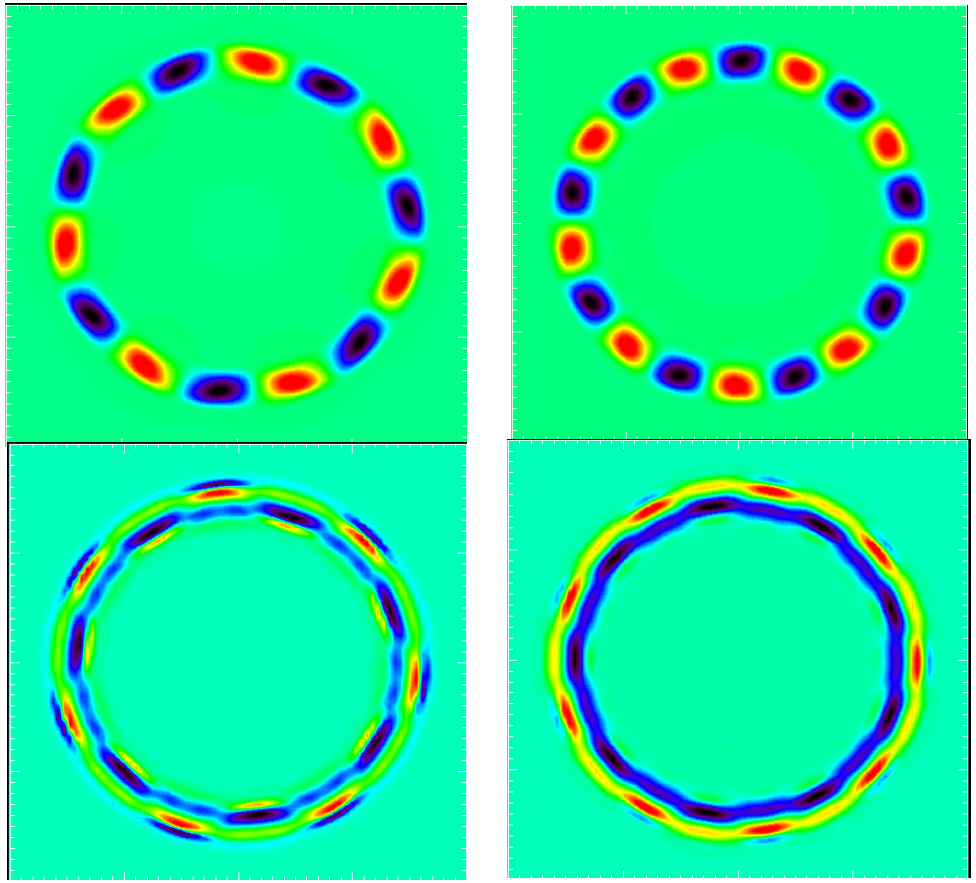

$\mathbf{V} = \nabla U \times \hat{z}$ $\mathbf{B} = \nabla \psi \times \hat{z} + B_0 \hat{z}$

Much more to do:

- Full MHD
- toroidal geometry
- more realistic ECCD source
- onset condition
- Compare with H. Park's diagnostic on KSTAR

M3D-C^1 Physics Studies in Progress

- Two-fluid reconnection in simple geometry
- Repeating sawtooth and stationary states
- Double tearing modes
- H-Mode pedestal formation
- Soft-beta limit and saturated modes
- Neoclassical tearing modes
- Disruption studies and resistive wall modes
- ELM studies and RMP
- NTV Studies
- LZ+JB Test problem

M3D-C^1 being used to study density pedestal formation from trans-sonic flow at plasma edge.

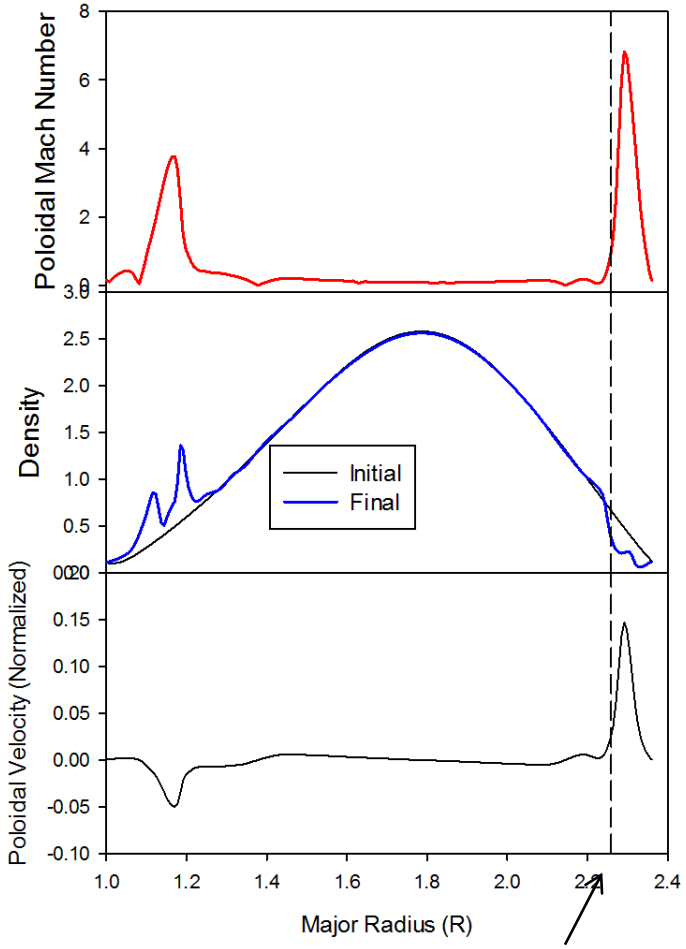

Radius where poloidal mach number: $M_P = 1$

We have added a poloidal force term in the momentum equation to model Er buildup due to orbit loss.

Steep density gradient forms in transonic flow region in agreement with theory and FLOW code

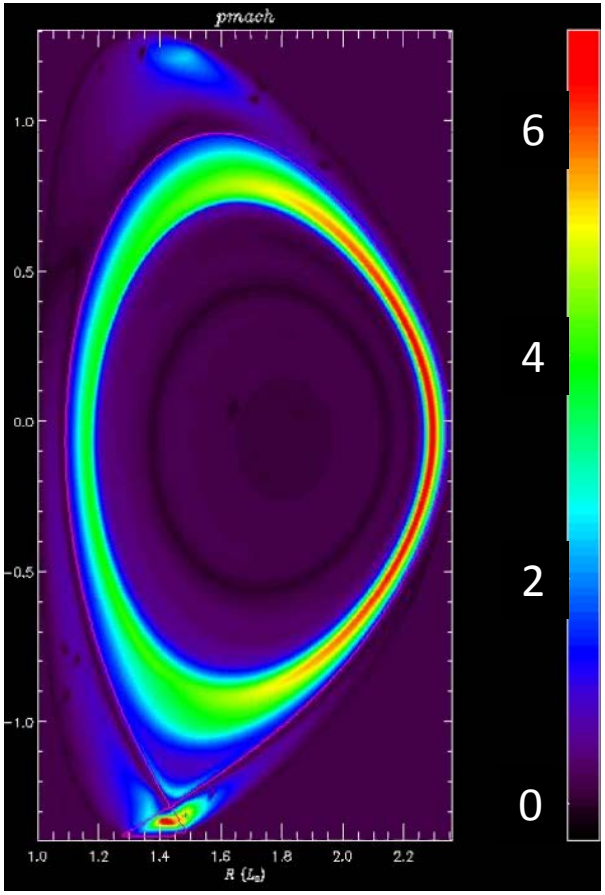

Poloidal Mach Number

with L. Guazzotto and R. Betti

M3D-C^1 Physics Studies in Progress

- Two-fluid reconnection in simple geometry
- Repeating sawtooth and stationary states
- Double tearing modes
- H-Mode pedestal formation
- Soft-beta limit and saturated modes
- Neoclassical tearing modes
- Disruption studies and resistive wall modes
- ELM studies and RMP
- NTV Studies
- LZ+JB Test problem

3D nonlinear simulation of NSTX with beam heating exceeding ideal MHD β-limit in center

As β-limit is exceeded in center, surfaces deform, become stochastic, & completely heal.

Net effect is"enhanced transport"

First pure n=3, then nonlinear, finally axisymmetric annulus

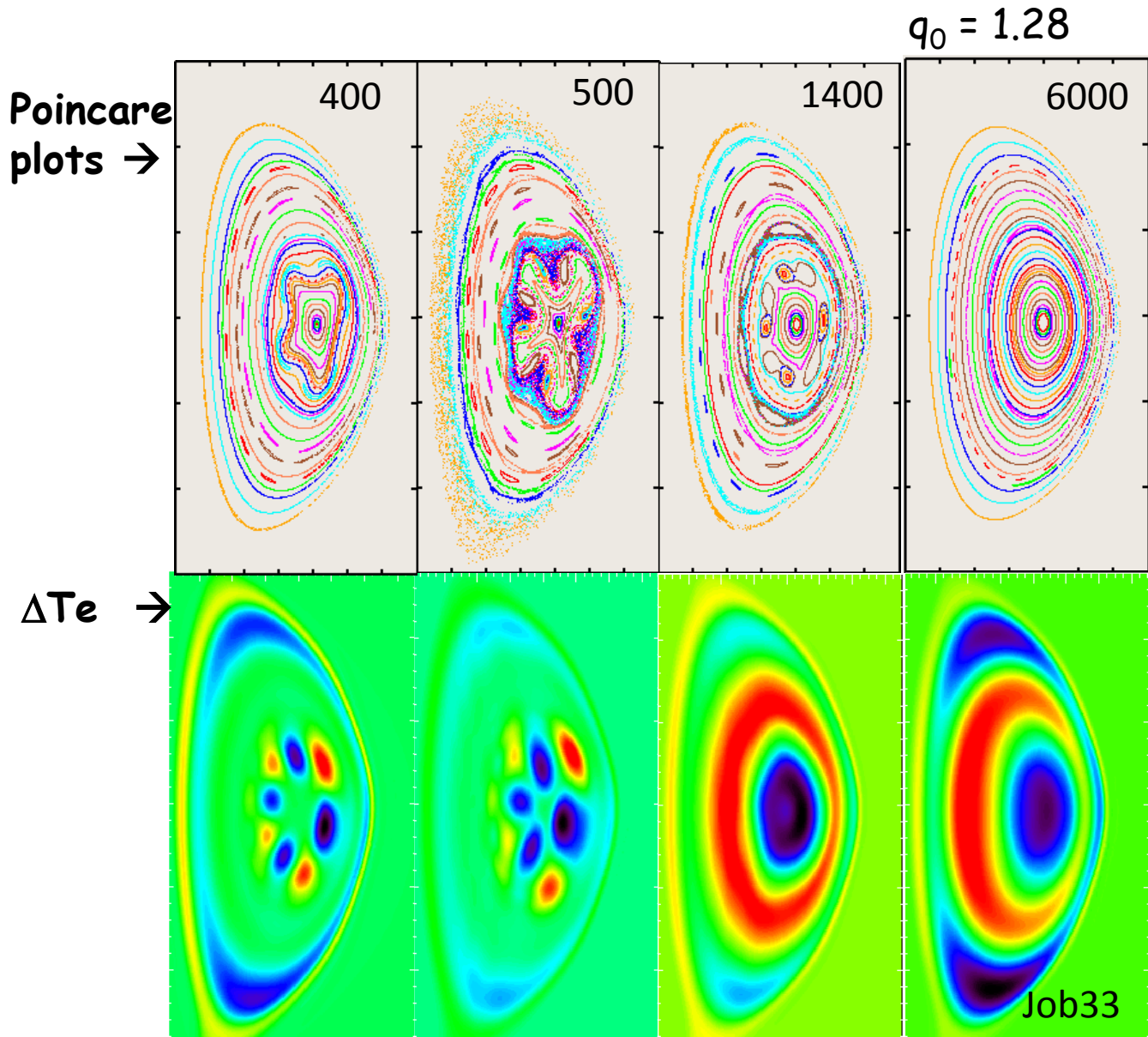

effect of increasing (decreasing) heating

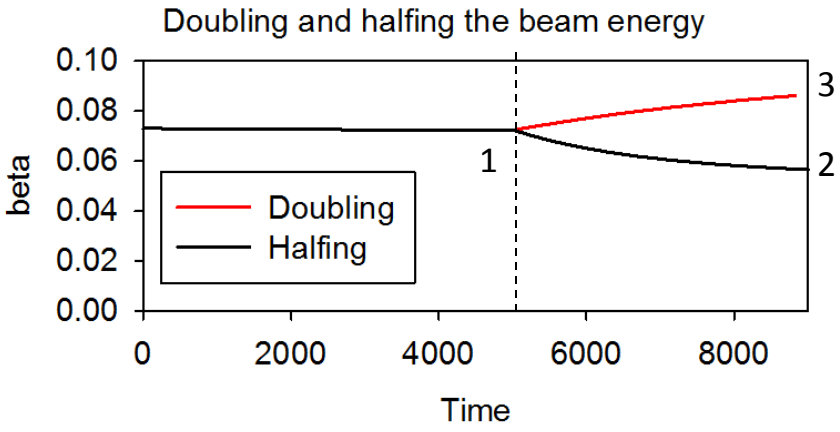

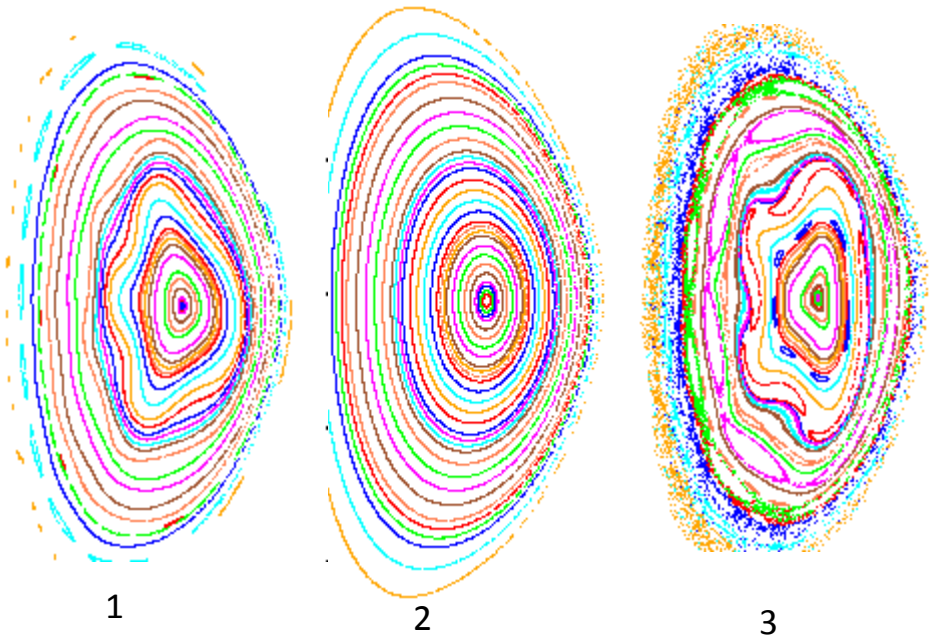

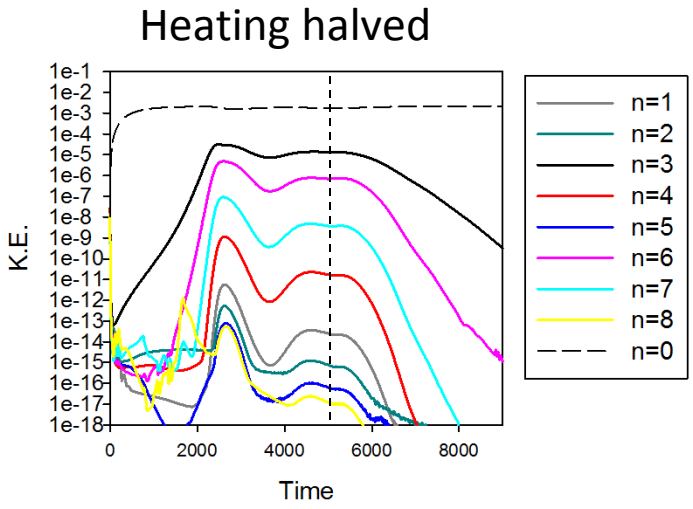

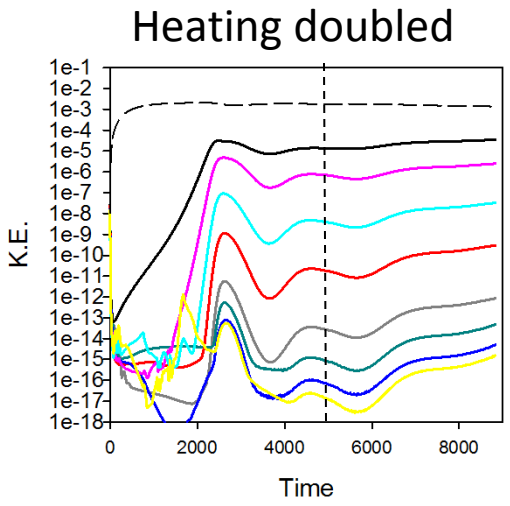

- With heating *reduced*, plasma returns to an axi-symmetric state (2)
- With heating *increased*, surfaces become more distorted, but still exhibits (reduced) confinement (3)

ITPA study of effect of internal (1,1) mode in ITER shows very small displacement of plasma boundary

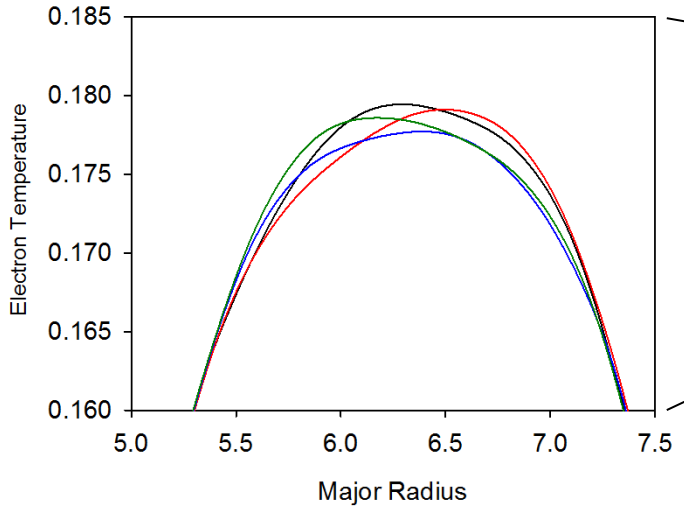

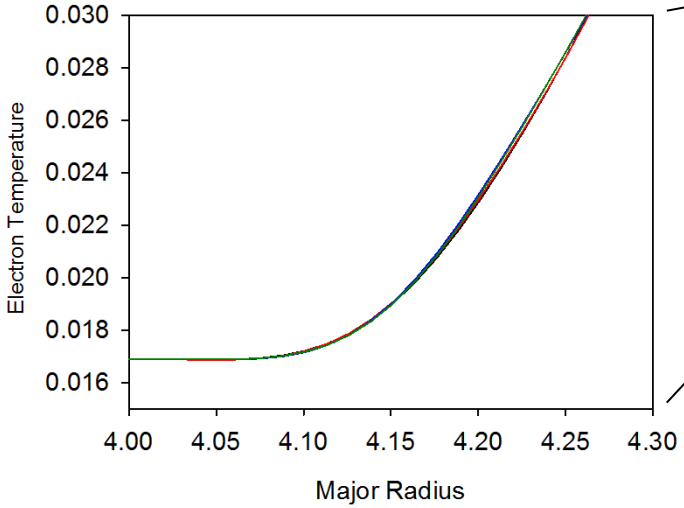

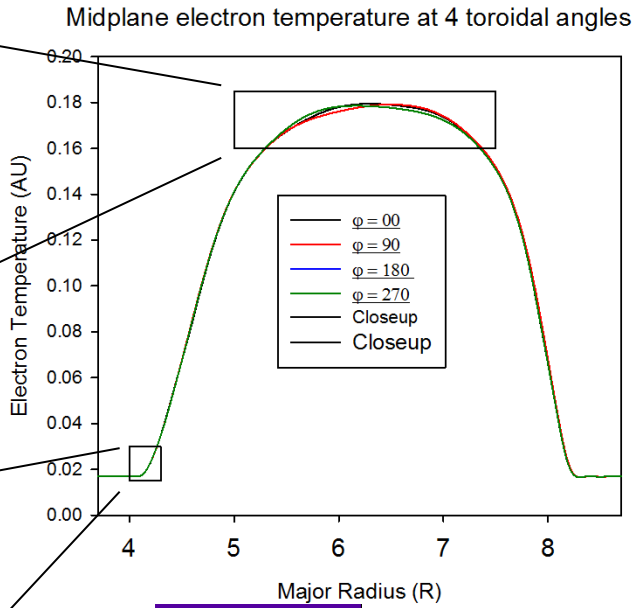

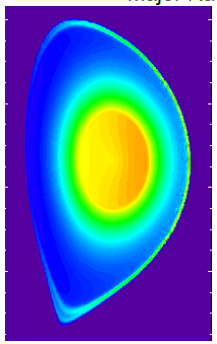

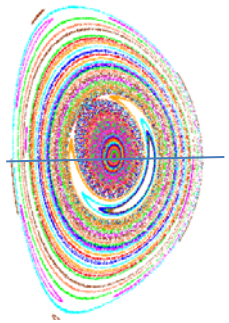

current Poincare

M3D-C^1 Physics Studies in Progress

- Two-fluid reconnection in simple geometry
- Repeating sawtooth and stationary states
- Double tearing modes
- H-Mode pedestal formation
- Soft-beta limit and saturated modes
- Neoclassical tearing modes
- Disruption studies and resistive wall modes
- ELM studies and RMP
- NTV Studies
- LZ+JB Test problem

Solve separately for the Maxwellian (M3D-C^1) and Non-Maxwellian parts of the distribution function

$$\frac{\partial \bar{f}_{NMe}}{\partial t} + v\left(\cos\chi\,\mathbf{b}\bullet\nabla\bar{f}_{NMe} + \frac{1}{2B}(\mathbf{b}\bullet\nabla B)\sin\chi\frac{\partial \bar{f}_{NMe}}{\partial\chi}\right)$$

$$+\frac{v_{the}^2}{n}\mathbf{b}\bullet\nabla n\left(\cos\chi\frac{\partial \bar{f}_{NMe}}{\partial v} - \sin\chi\frac{1}{v}\frac{\partial \bar{f}_{NMe}}{\partial\chi}\right) = \{S(\chi,\theta,v)\}f_{Me} + \left\langle C_{ee}\left[f_e,f_e\right] + C_{ei}\left[f_e,f_i\right]\right\rangle$$

$$S(\chi,\theta,v) = \cos\chi\frac{v}{2T_e}\left(5-\frac{v^2}{v_{the}^2}\right)\mathbf{b}\bullet\nabla T_e + \cos\chi\frac{v}{nT_e}\mathbf{b}\bullet\left[\frac{2}{3}\nabla\left(p_{e\|}-p_{e\perp}\right) - \left(p_{e\|}-p_{e\perp}\right)\frac{1}{B}\nabla B - F_e^{coll}\right]$$

$$+P_2(\cos\chi)\frac{v^2}{3v_{the}^2}\left(\nabla\bullet\mathbf{u}_e - 3\mathbf{b}\bullet\left[(\mathbf{b}\bullet\nabla)\mathbf{u}_e\right]\right) + \frac{1}{3nT_e}\left(\frac{v^2}{v_{the}^2}-3\right)\left[\nabla\bullet\left(q_{e\|}\mathbf{b}\right) - G_e^{coll}\right]$$

$$+\frac{1}{6eB}\left[2P_2(\cos\chi)\frac{v^2}{v_{the}^2}\left(\frac{v^2}{v_{the}^2}-5\right) + \frac{v^4}{v_{the}^4} - 10\frac{v^2}{v_{the}^2} + 15\right](\mathbf{b}\times\boldsymbol{\kappa})\bullet\nabla T_e$$

$$+\frac{1}{6eB}\left[-P_2(\cos\chi)\frac{v^2}{v_{the}^2}\left(\frac{v^2}{v_{the}^2}-5\right) + \frac{v^4}{v_{the}^4} - 10\frac{v^2}{v_{the}^2} + 15\right]\frac{1}{B}(\mathbf{b}\times\nabla B)\bullet\nabla T_e + P_2(\cos\chi)\frac{v^2}{3eBv_{the}^2}\frac{1}{n}(\mathbf{b}\times\nabla n)\bullet\nabla T_e$$

The first 3 velocity moments of f_{NMe} vanish

$\mathbf{b},\mathbf{u}_e,B,T_e,T_i,n\}$ These come from the M3D-C^1 code.

$$\left.\begin{aligned}\left(p_{e\|}-p_{e\perp}\right) &= 2\pi m_e\int_0^\infty dv\,v^4\int_0^\pi d\chi\,\sin\chi\,P_2(\cos\chi)\bar{f}_{NMe}\\ \hat{F}_{e\|}^{coll} &= -2\pi m_e\nu_e v_{the}^2\int_0^\infty dv\int_0^\pi d\chi\,\sin\chi\cos\chi\,\bar{f}_{NMe}\end{aligned}\right\}$$

These are used in M3D-C^1 to close equations

with B. Lyons and J. Ramos

The kinetic solver has been implemented and benchmarked in axisymmetric geometry.

$$\langle \mathbf{J} \bullet \mathbf{B} \rangle = \sigma_{neo} \langle \mathbf{E} \bullet \mathbf{B} \rangle - cI \left[L_{31} \frac{dP}{d\psi} + L_{32} n_e \frac{dT_e}{d\psi} + \alpha L_{34} n_i \frac{dT_i}{d\psi} \right]$$

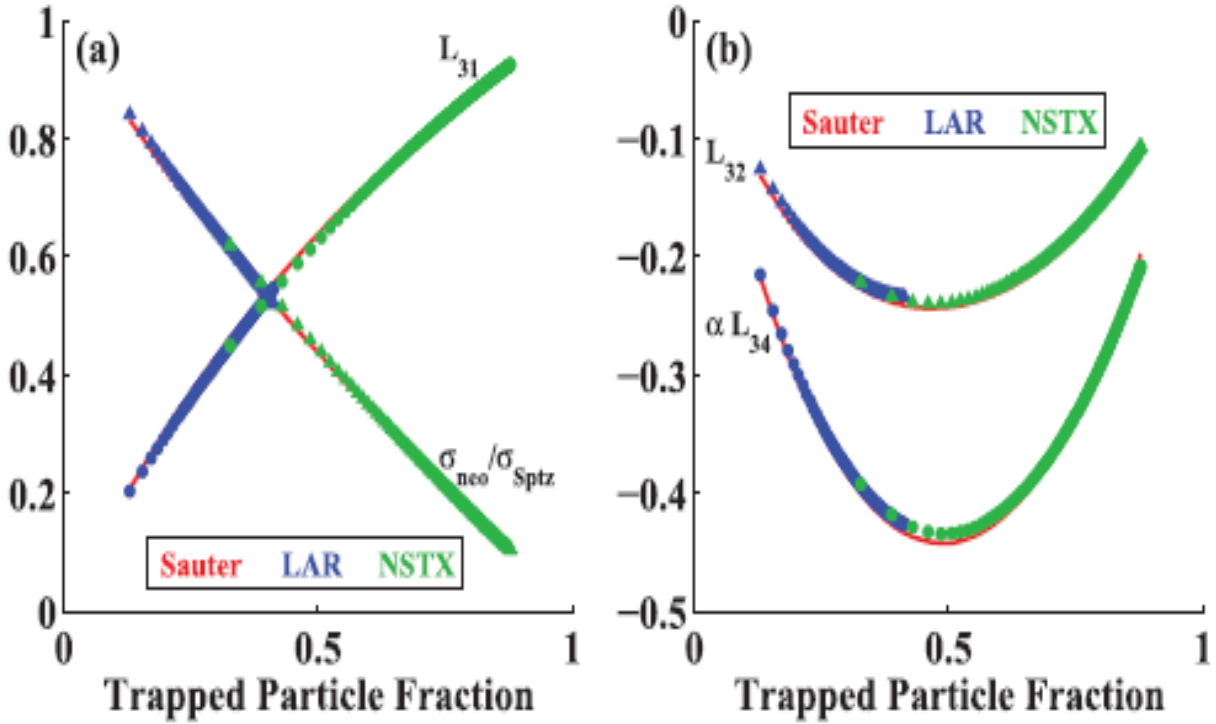

- Very good agreement with Sauter model in axisymmetric limit
- further benchmarking in all collisionality regimes has been done
- Initial coupling to MHD code has been done and presented at Sherwood 2014 by B. Lyons

M3D-C^1 Physics Studies in Progress

- Two-fluid reconnection in simple geometry
- Repeating sawtooth and stationary states
- Double tearing modes
- H-Mode pedestal formation
- Soft-beta limit and saturated modes
- Neoclassical tearing modes
- Disruption studies and resistive wall modes
- ELM studies and RMP
- NTV Studies
- LZ+JB Test problem

*M3D-C^1 has been extended to 3 regions for RW**

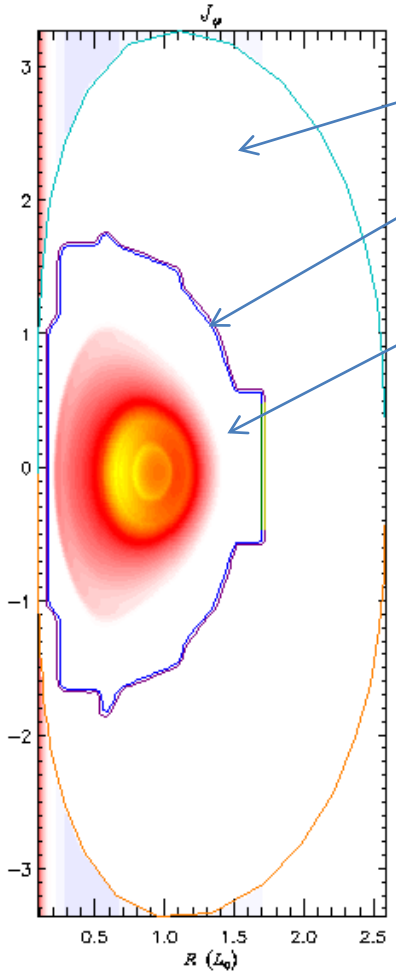

Vacuum (**J**=0)

RW (**E** = η_W **J**)

Plasma (X-MHD)

BC:

- **v**, p, n set at inner wall
- **B** set at outer (ideal) wall

- No boundary conditions on **B** or **J** at the resistive wall
- Current can flow into and through the wall

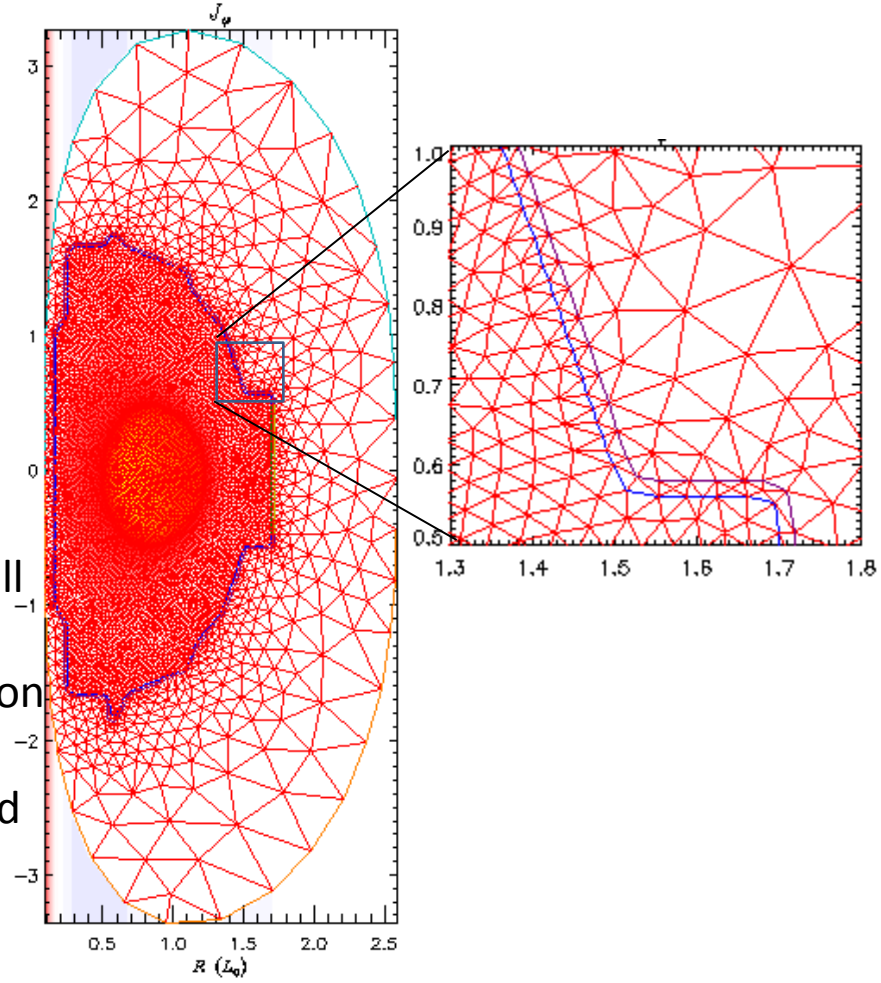

*Ferraro, Sherwood and CEMM: 2014

Initial simulation of VDE in NSTX with M3D-C¹

- Initial results from 2D low-resolution calculation
- Both Positive and Negative (counter-current) currents are found
- Now extending these results to 3D and realistic η_W and 3D RWM

Toroidal current density at 5 times in VDE simulation

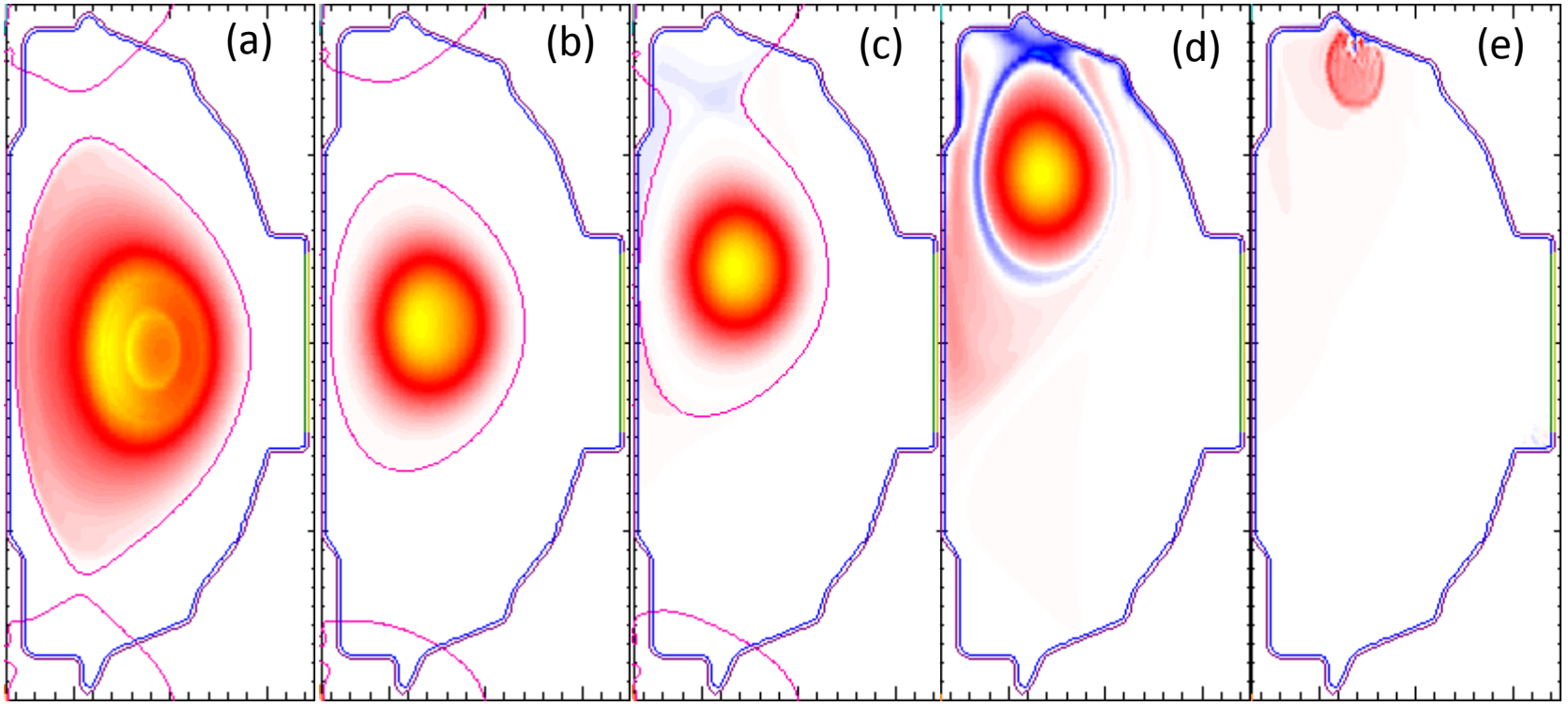

M3D-C^1 J_φ, p, and I=RB$_T$ at a late time

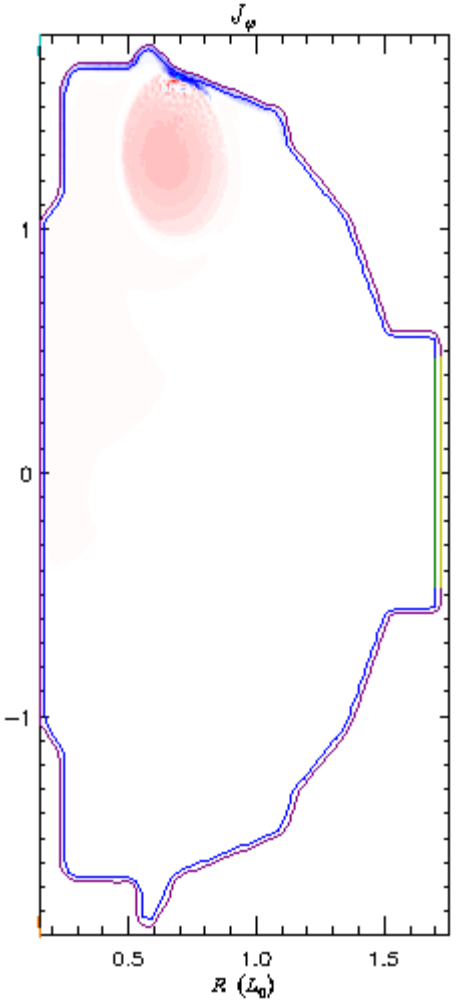

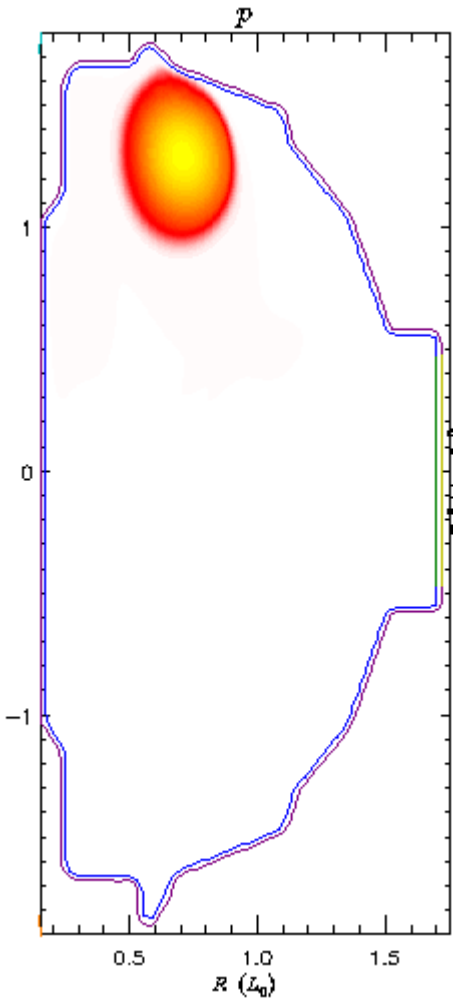

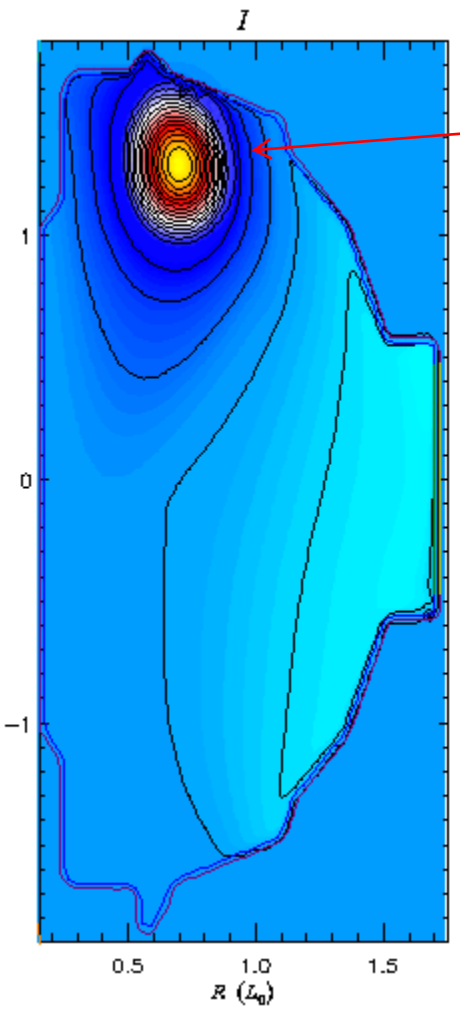

Note halo currents

Dependence of NSTX VDE on η_W

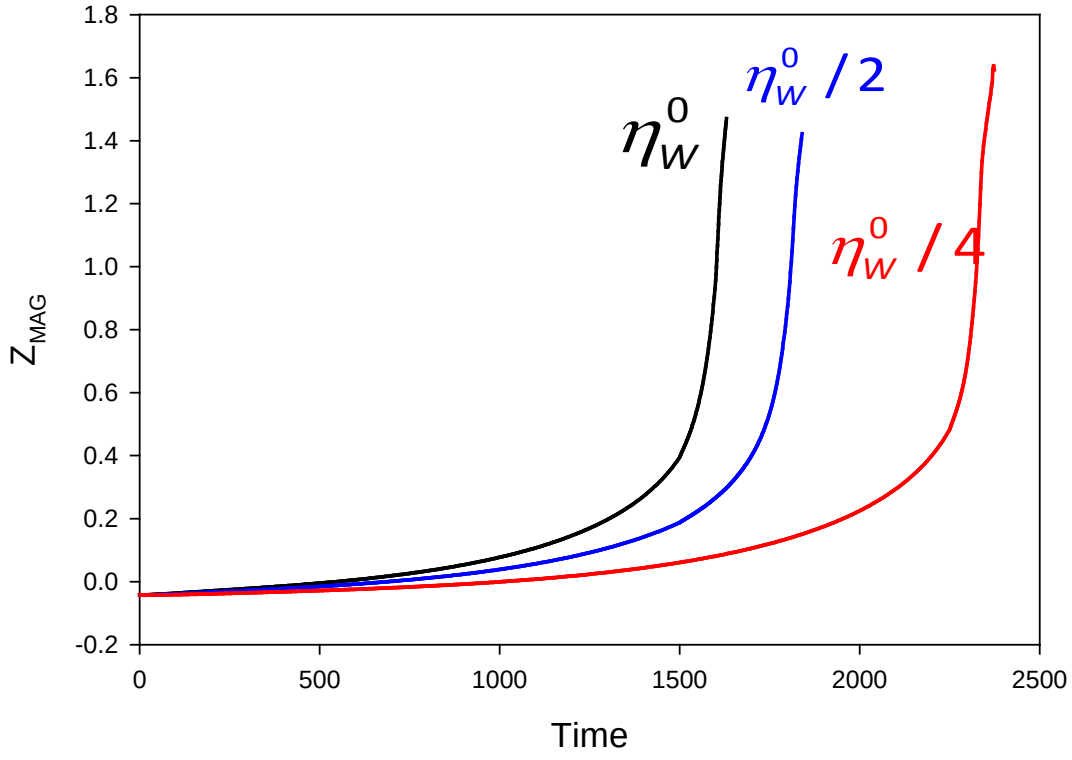

Growth rate scales inversely with wall resistivity η_W as expected

Disruption studies during current rampdown in NSTX - 1

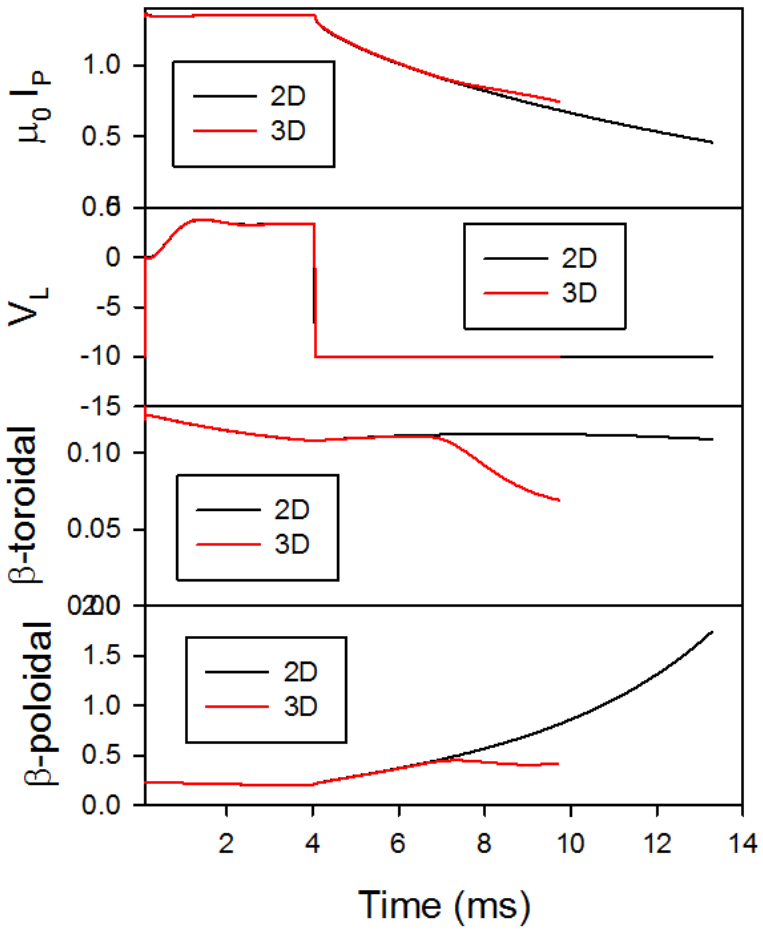

- At the end of the discharge, the loop voltage in NSTX is rapidly reversed to quench the OH coils
- Experimentally, this often leads to a disruption
- We are trying to reproduce this with M3D-C^1 using realistic parameters
- Difference in 2D and 3D behavior is due to 3D instabilities.
- Will this lead to a disruption?

Disruption studies during current rampdown in NSTX - 2

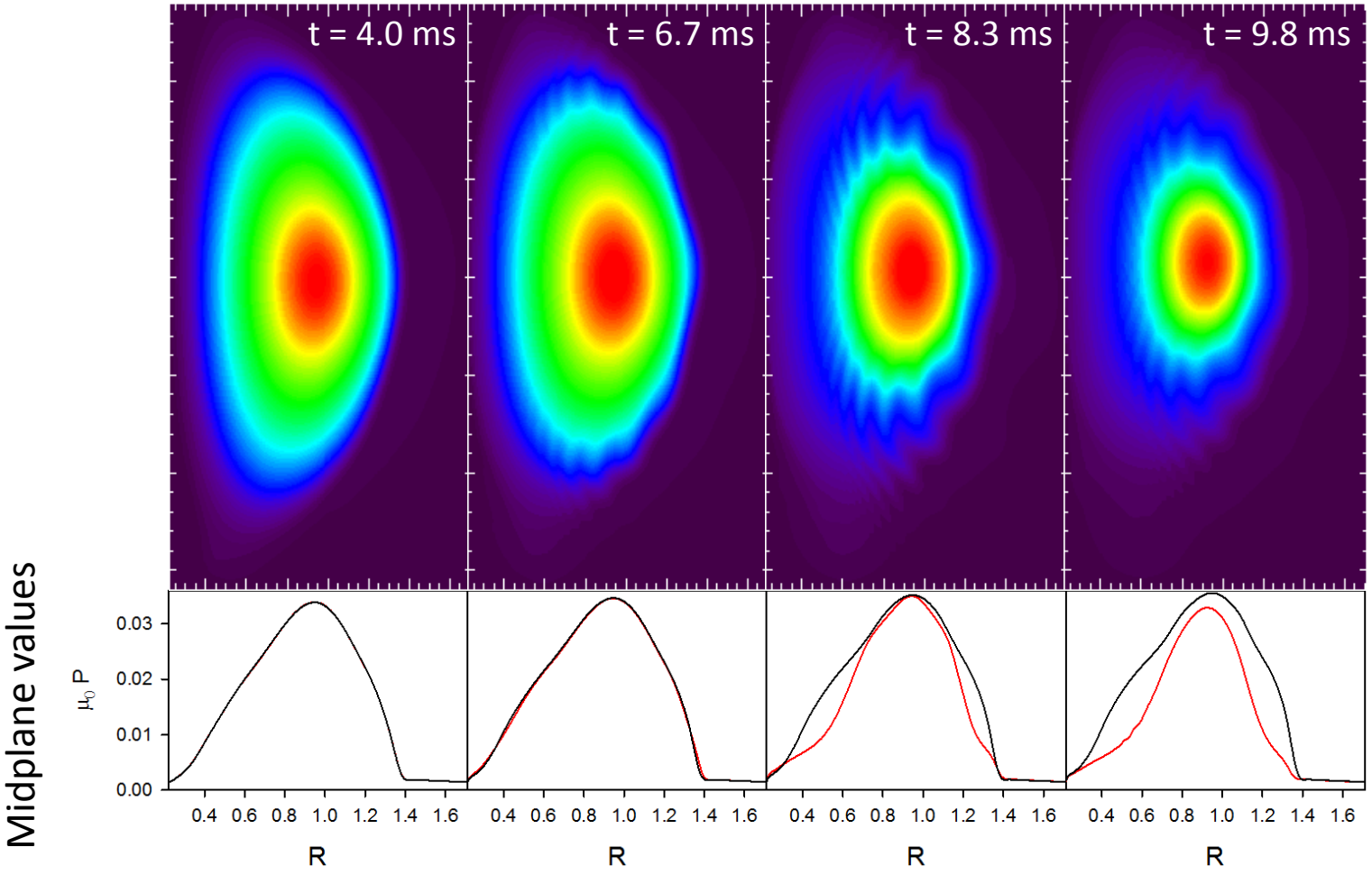

Pressure in 2D (black) and 3D (red) at 4 times

Disruption studies during current rampdown in NSTX - 3

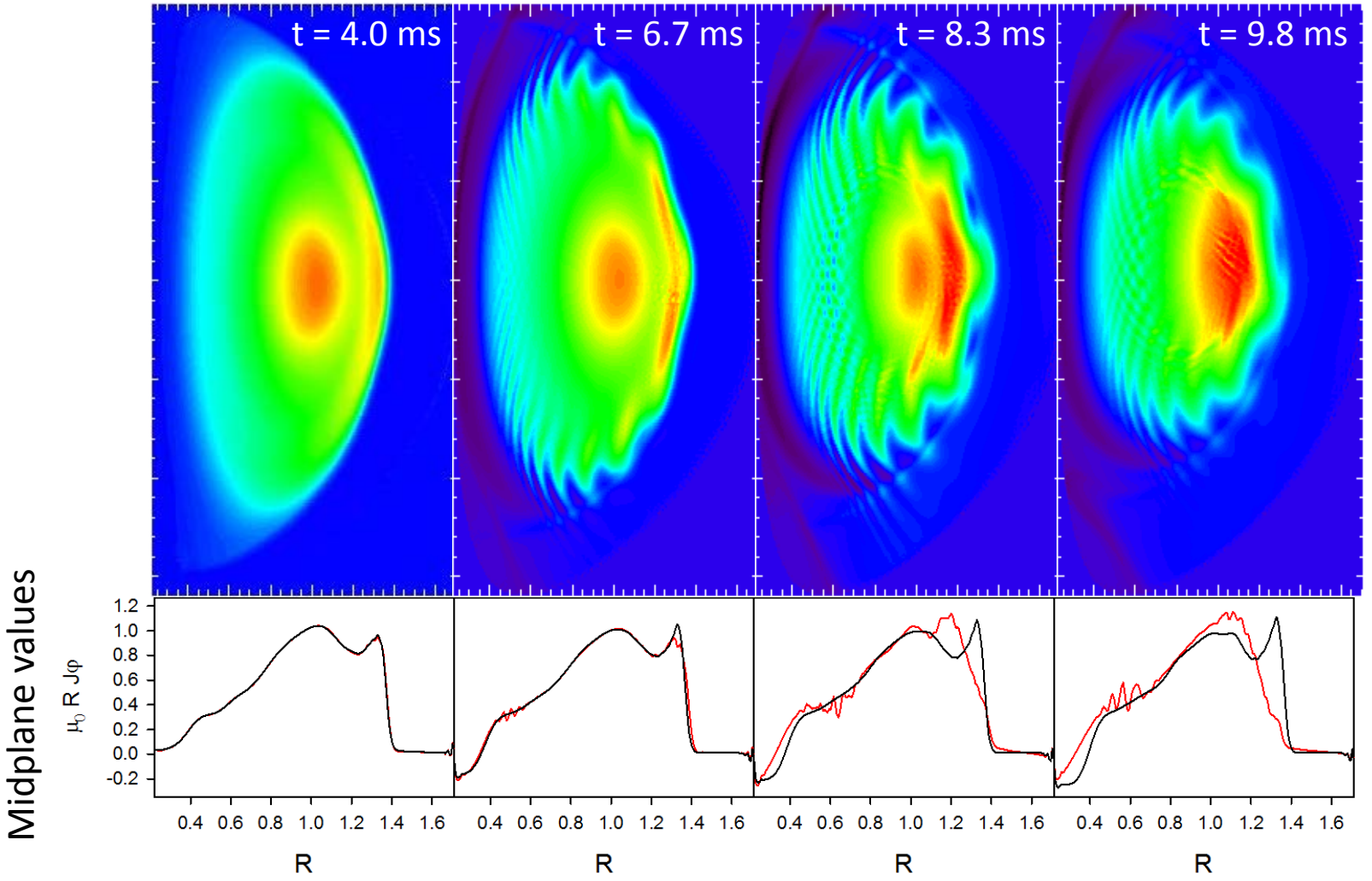

Toroidal current density in 2D (black) and 3D (red) at 4 times

M3D-C^1 Physics Studies in Progress

- Two-fluid reconnection in simple geometry
- Repeating sawtooth and stationary states
- Double tearing modes
- H-Mode pedestal formation
- Soft-beta limit and saturated modes
- Neoclassical tearing modes
- Disruption studies and resistive wall modes
- ELM studies and RMP
- NTV Studies
- LZ+JB Test problem

ELM Studies-simple geometries

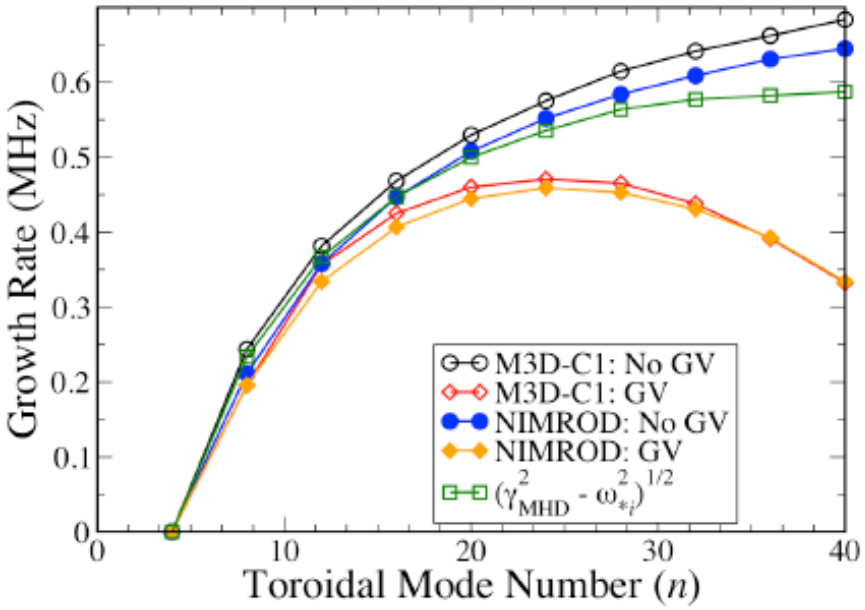

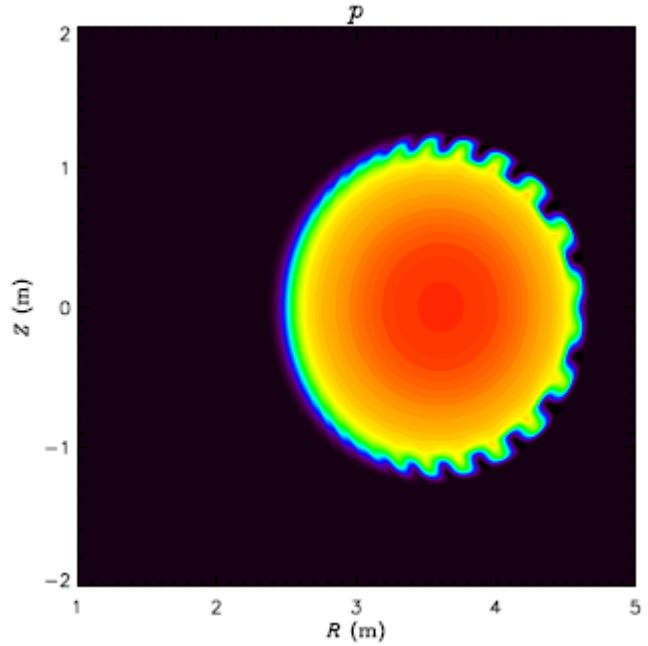

- Benchmark of M3D-C^1 and NIMROD with/wo gyroviscosity

- Both codes show stabilization much greater than the $\omega_{*i}/2$ approximation

Nonlinear 2-fluid benchmark underway:

- full 8-field two-fluid model
- Spitzer resistivity S = 1.5 x 10^9 in center
- realistic anomalous transport

ELM Studies-2

- M3D-C^1 is being used by DIII-D to interpret soft-x-ray signals during RMP experiments

- Fields from M3D-C^1 (which include plasma response) are being used by SPIRAL code to calculate effect of RMP fields on particle orbits

Experimental data

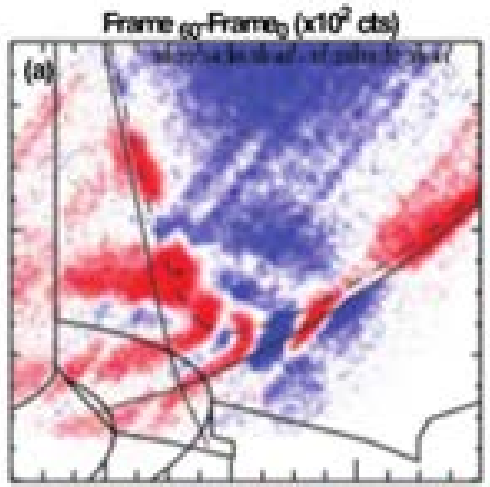

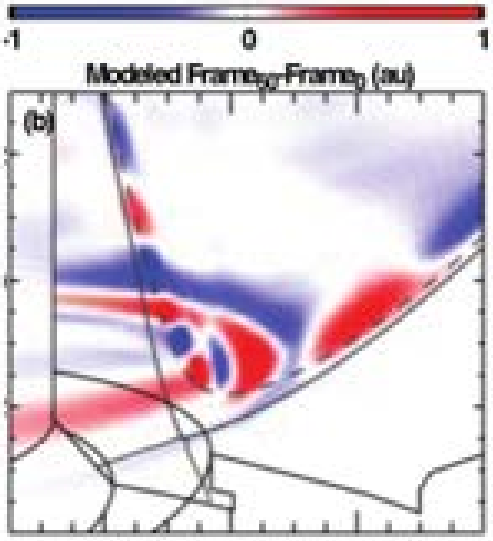

M3D-C^1 synthetic diagnostic

ELM Studies-3

- Code benchmarking is also underway on an actual DIII-D shot of interest

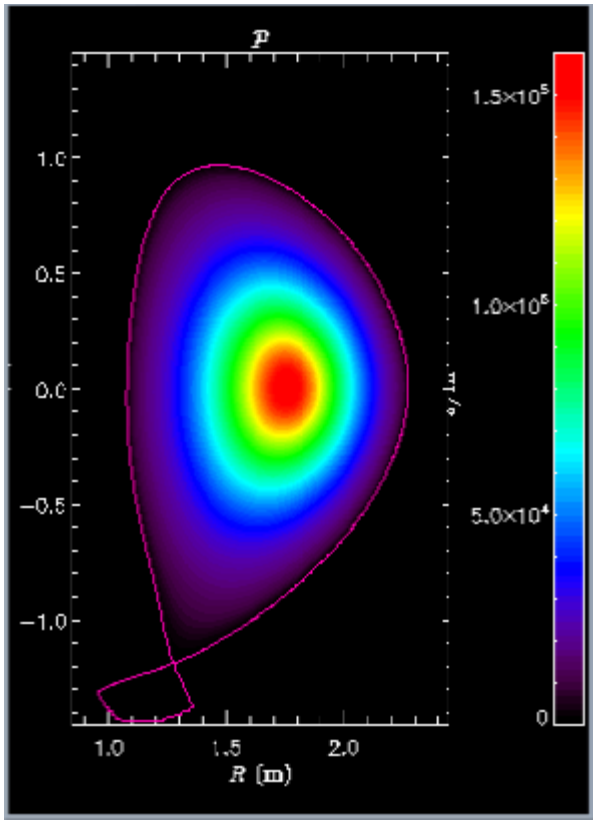

n=10 n=5

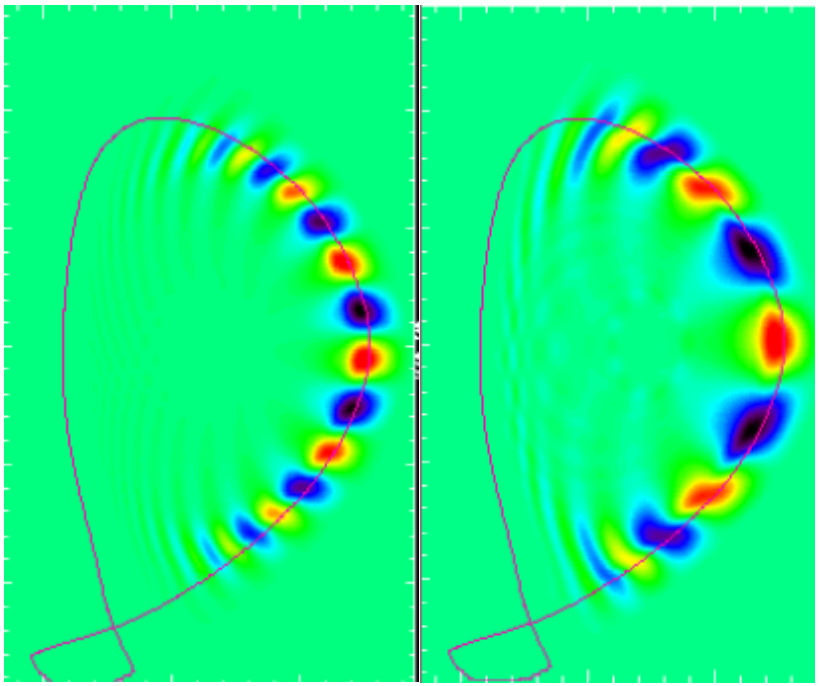

This time slice is ideal MHD stable but unstable to resistive ballooning modes

M3D-C^1 Physics Studies in Progress

- Two-fluid reconnection in simple geometry
- Repeating sawtooth and stationary states
- Double tearing modes
- H-Mode pedestal formation
- Soft-beta limit and saturated modes
- Neoclassical tearing modes
- Disruption studies and resistive wall modes
- ELM studies and RMP
- NTV Studies
- LZ+JB Test problem

Neoclassical Toroidal Viscosity

Control of the plasma rotation profile by applying 3D fields depends on torques generated by neoclassical toroidal viscosity

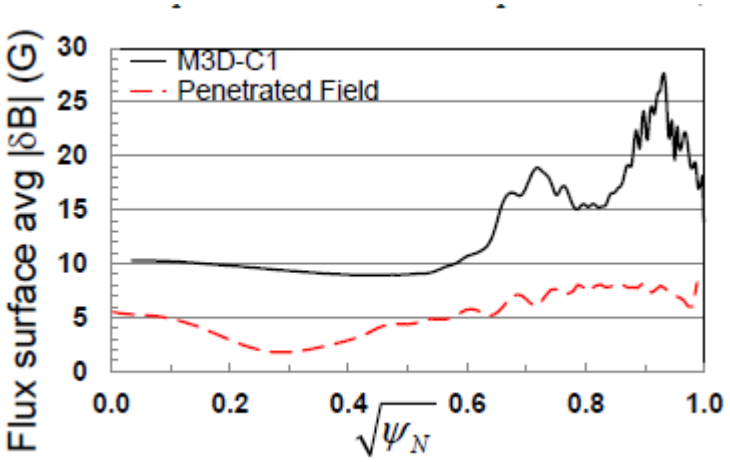

Flux-surface averaged |δB| for fully-penetrated field model and the M3D-C^1 single fluid model

- Present work[1] uses M3D-C^1 fields and evaluates torque using NTVTOK code
- Future work will use the M3D-C^1 kinetic formulation to evaluate the torque self-consistently
- Much data exists on NSTX and KSTAR for comparison.

[1]S. Sabbagh, et al. "Physical Characteristics of Neoclassical Toroidal Viscosity in Tokamaks for Rotation Control and the Evaluation of Plasma Response, IAEA 2014

M3D-C^1 Physics Studies in Progress

- Two-fluid reconnection in simple geometry
- Repeating sawtooth and stationary states
- Double tearing modes
- H-Mode pedestal formation
- Soft-beta limit and saturated modes
- Neoclassical tearing modes
- Disruption studies and resistive wall modes
- ELM studies and RMP
- NTV Studies
- LZ+JB Test problem

LZ+JB Test problem

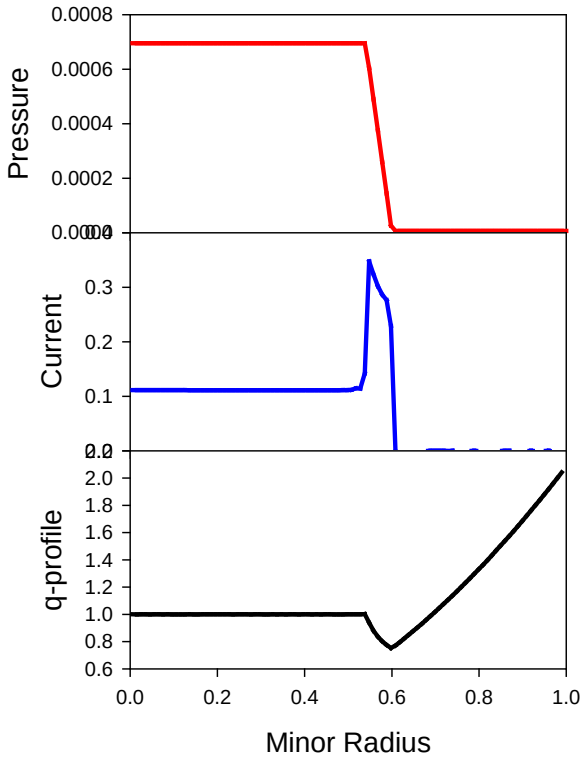

Cylindrical equilibrium presented by Breslau at Sherwood 2014

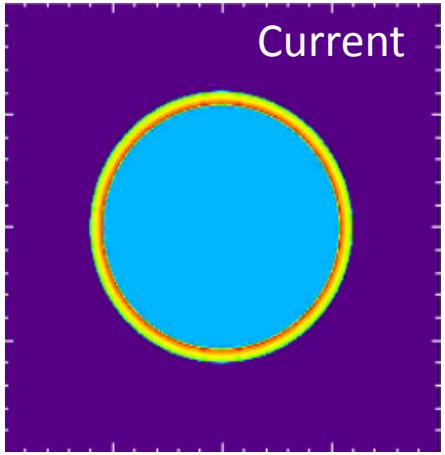

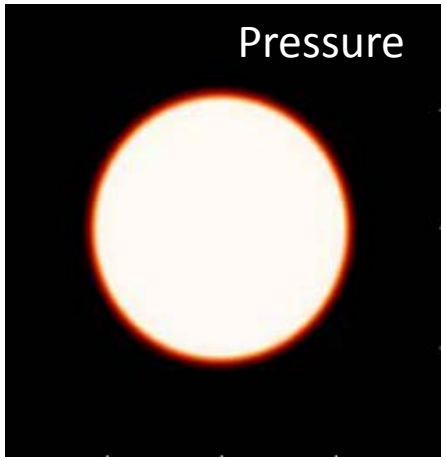

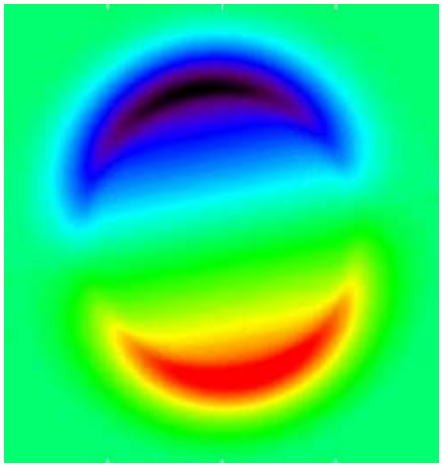

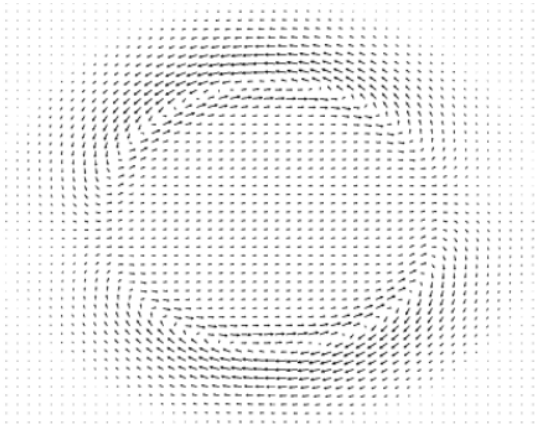

Linear (1,1) eigenmode: stream-function and velocity vectors

LZ+JB Test problem

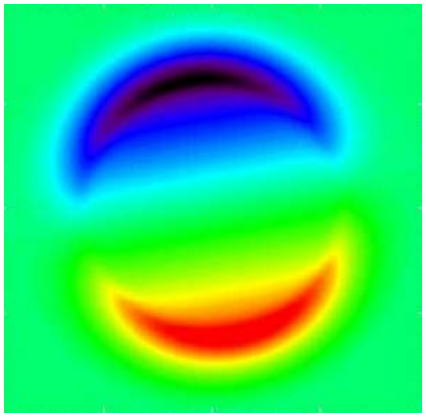

n=1, m=1, γ= 0.025

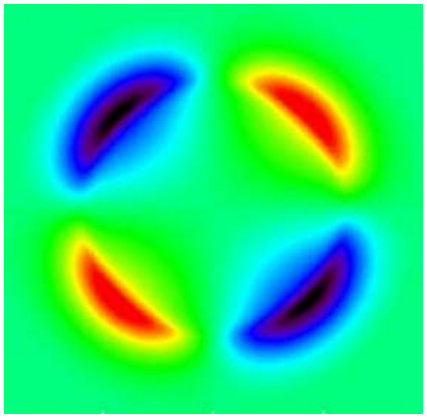

n=2, m=2, γ= 0.035

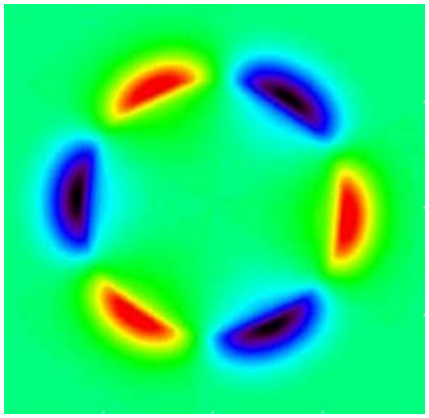

n=3, m=3, γ= 0.036

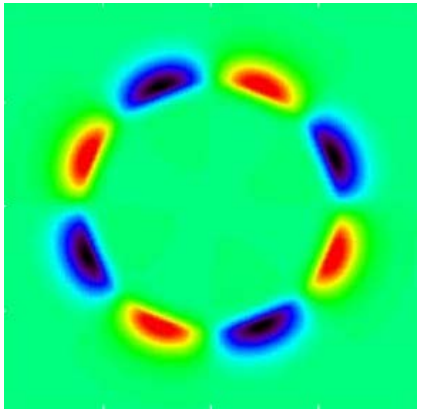

n=4, m=4, γ= 0.026

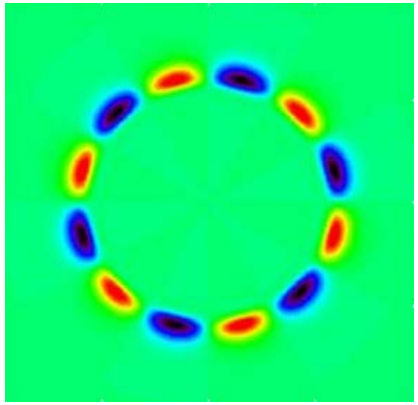

n=7, m=6, γ= 0.018

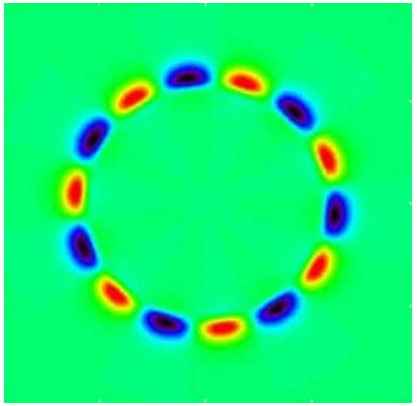

n=8, m=7, γ= 0.024

Equilibrium is linearly unstable to many modes!

LZ+JB Test problem

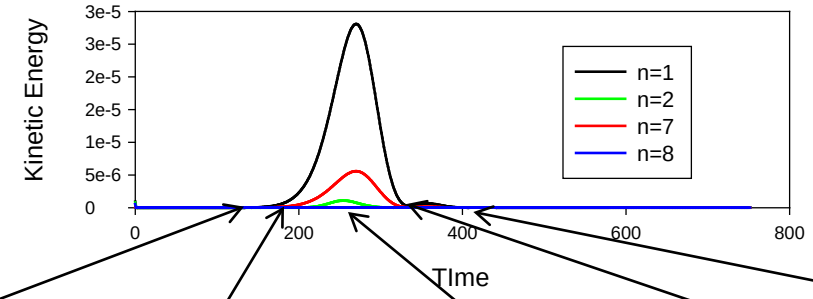

ΔJ

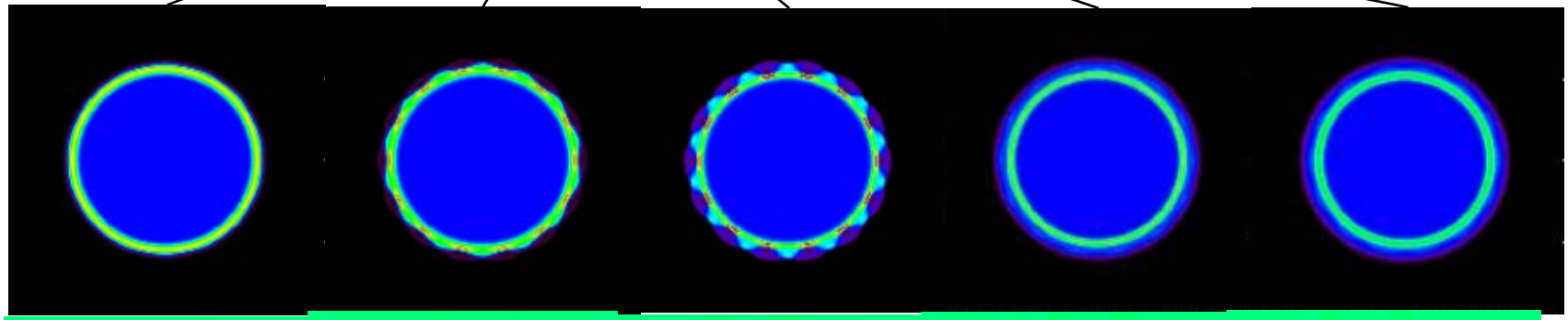

U

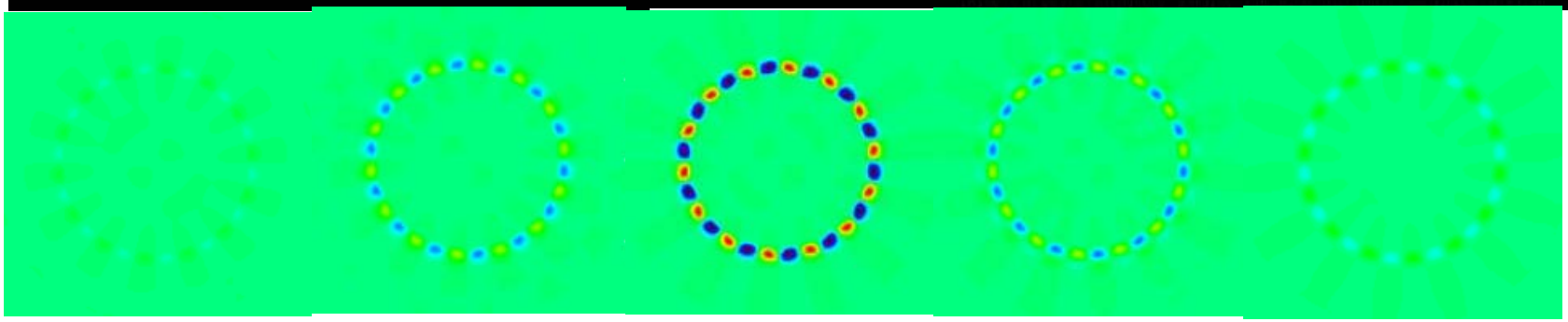

Starting from random initial conditions, an initial mode with many harmonics grows up and saturates, slightly changing the profiles.

LZ+JB Test problem

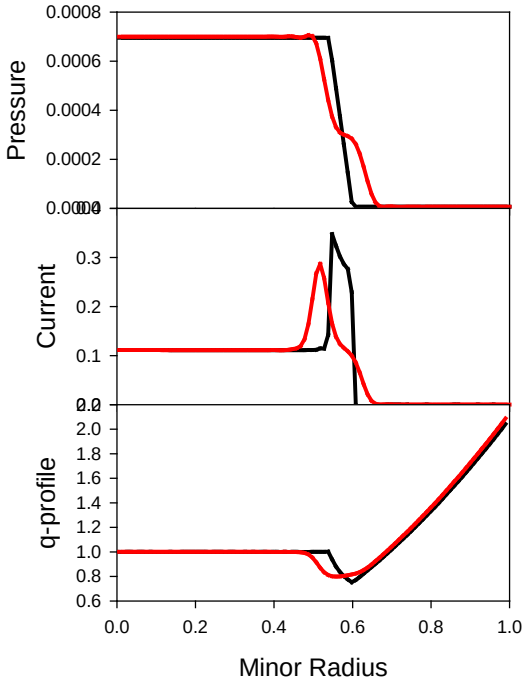

Initial nonlinear event lasting ~ 100 τ_A modifies current and pressure profiles

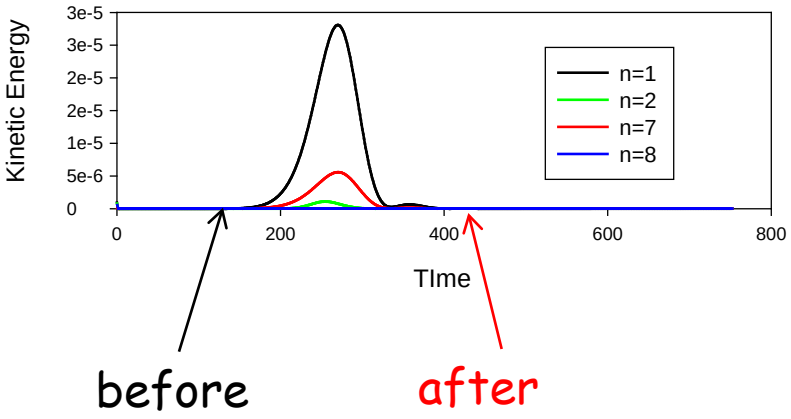

This is still being run nonlinearly to see if the (1,1) mode develops as expected. Initial (1,1) perturbation may be too small.

M3D-C^1 Future Plans

Physics Studies

- Disruption forces on vessel with realistic parameters
  - Benchmark 2D runs with TSC
- More on thermal quench, ELMs, EHO: experimental validation
- More on sawteeth: experimental validation
- Error fields and mode locking
- Radiation physics and snakes
- Complete kinetic coupling for NTM, NTV & ST
- Runaway electrons during disruptions
  - Extend TSC model to 3D

Code Capabilities

- Ability to switch modes: 2D →3D linear → 3D nonlinear
- Diagnostic to calculate magnetic island width (Hudson)
- Improve parallel scaling of iterative solve for fields
- Improve single processor performance (GPUs?)
- Add energetic particles ?

Extra Viewgraphs

Viscosity Scan at constant $S=10^6$ and $\beta=.001$

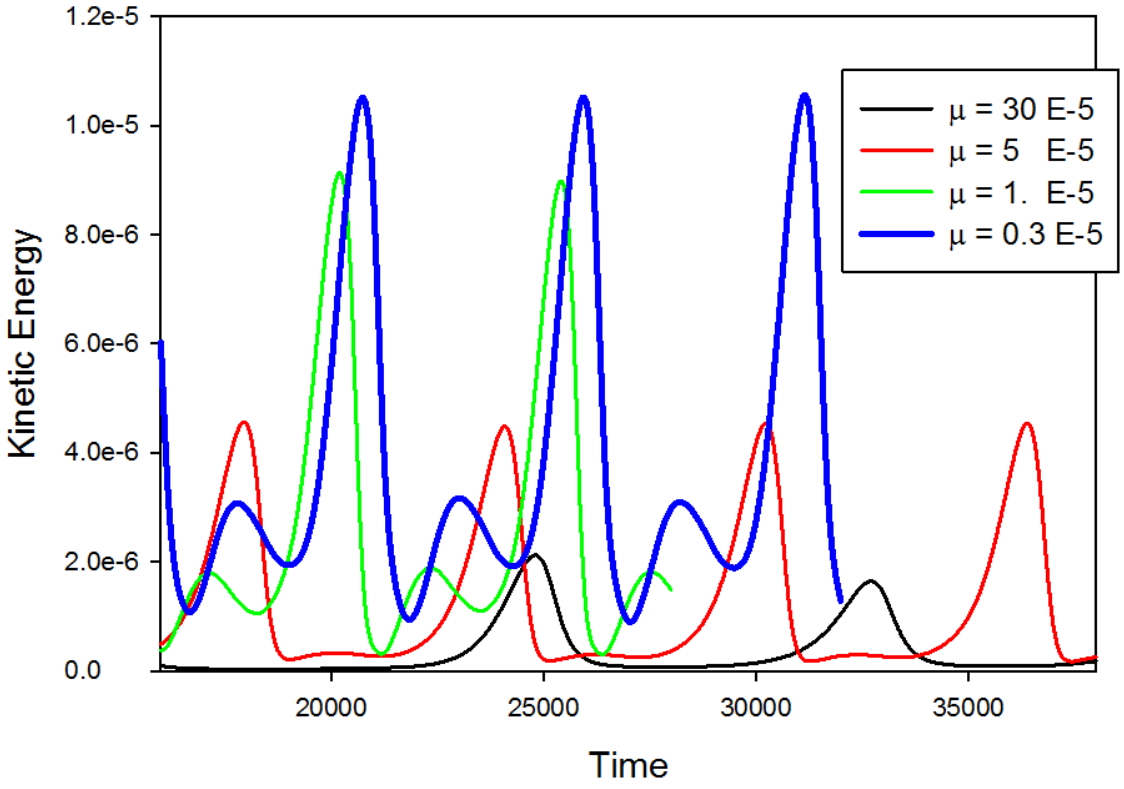

- Max KE amplitude increases with μ^{-1} (to a point)
- Period increases with μ
- Lowest μ can have more complex behavior (bouncing)

CMOD08
CMOD10
CMOD26
CMOD30

Adding sheared rotation causes oscillations to reappear

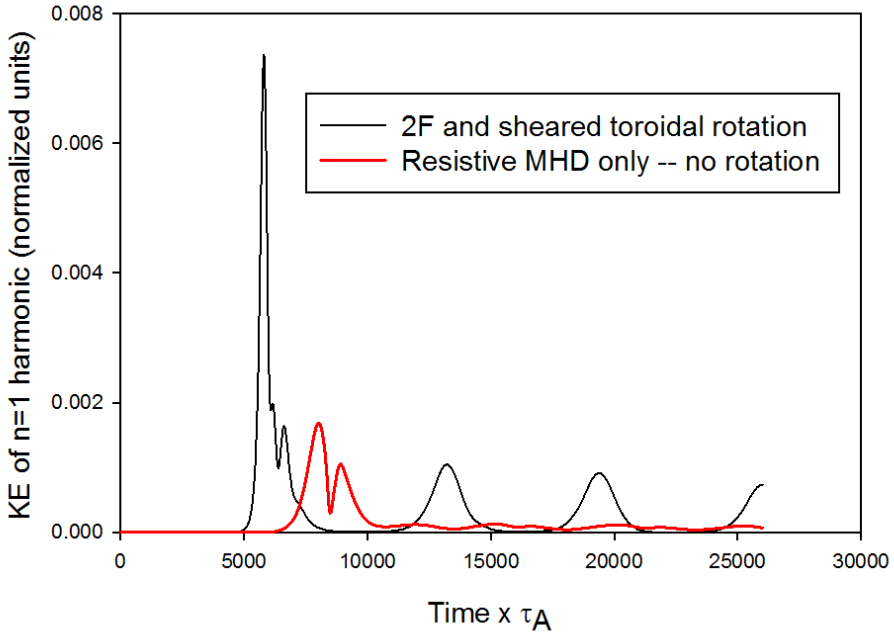

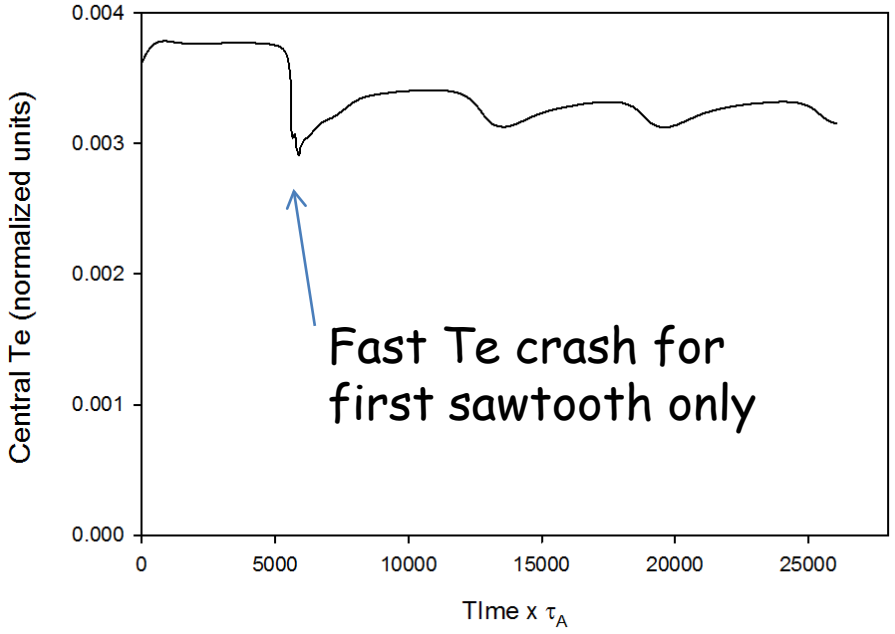

- Comparison of two runs with same β = 0.5% and same η=1.4E-6

- Two-fluid (TF) terms lead to faster initial crash, but not faster repeated crashes

- In this case, oscillations eventually died out

CMOD37G
CMOD011

We have performed comprehensive studies of runaway generation in ITER (in 2D) and how to control them

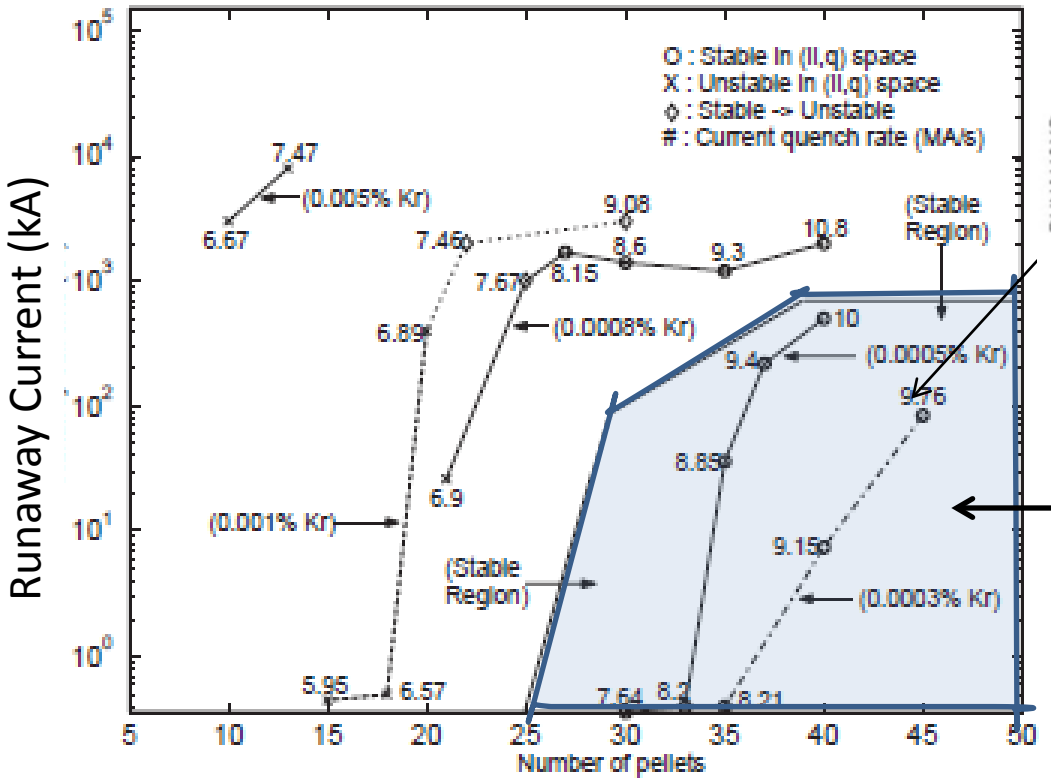

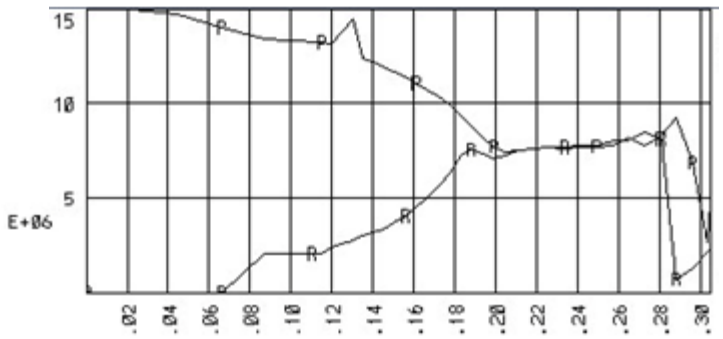

A regime exists where the plasma remains MHD stable during 4-sec current rampdown with negligible runaway generation

- 4 sec current ramp-down using PF coils
- Sequence of Krypton doped hydrogen pellets
- Monitor MHD stability

A fast shutdown technique for large tokamaks: NF 40 923 (2000)

Detailed Modeling of NSTX VDE with TSC code

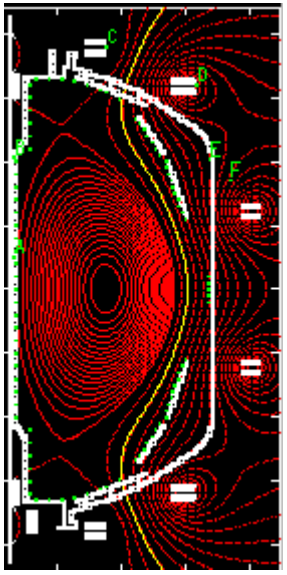

259 ms

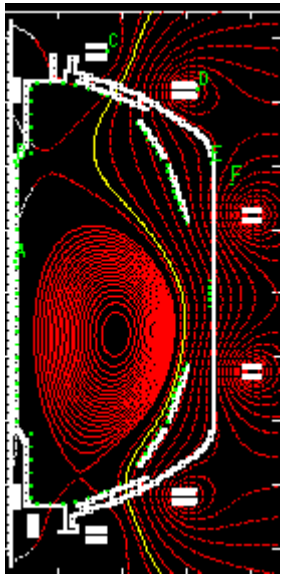

300 ms

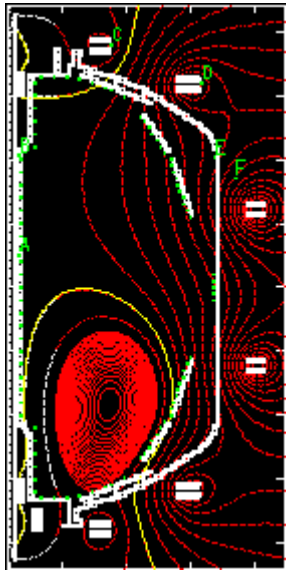

310 ms

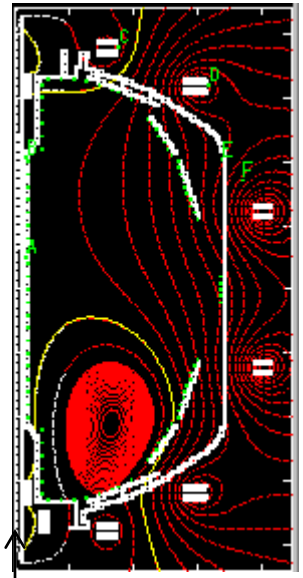

311 ms

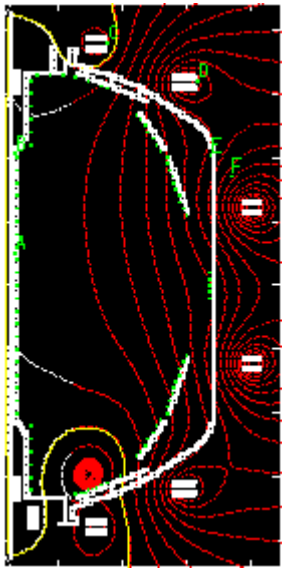

312 ms

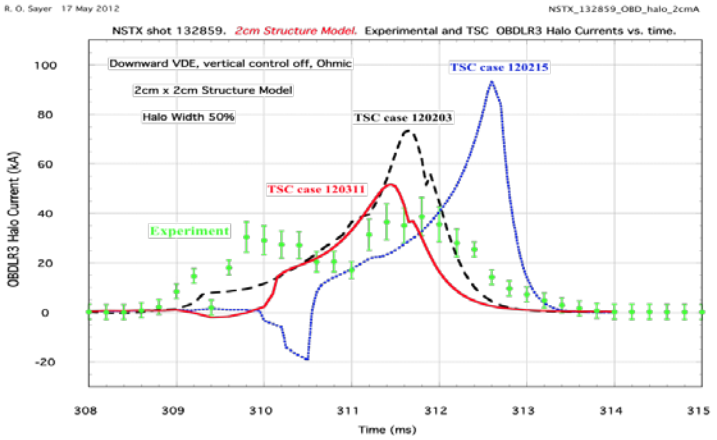

q_{95} ~ 2

q_0 ~ 1.2

Thermal quench & start of current quench

T_{HALO} ~ 6-10 eV

TQ: large $\chi_\perp$

Te: keV → 30ev in ~ < .1ms

CQ: ~ 2-3 ms.

Resistive decay in cold plasma

With R. Sayer, S. Gerhardt

➔ *Resistive MHD leads to scaling that is inconsistent with experiment!*

Change in q_0 between sawteeth: $\Delta q_0 = \eta\, \Delta t$

displacement due to resistive MHD: $\xi = \xi_0 e^{\gamma\, \Delta t}$

if $\gamma \sim \eta^{1/3}$, time for N e-foldings: $\Delta t = \frac{N}{\gamma} \sim \eta^{-1/3}$

$$\Delta q_0 = \eta\, \Delta t \sim \eta^{2/3} \to 0 \text{ as } \eta \to 0$$